NOSC TR 923
Revision A

NAVAL OCEAN SYSTEMS CENTER San Diego, California 92152-5000

(12)

NOSC TR 923
Revision A

Technical Report 923
Revision A (May 1986)
October 1983
Final Report

Surface-Search Radar Performance in the Evaporation Duct: Global Predictions

K. D. Anderson

"Original contains color plates: All DTIC reproductions will be in black and white"

Superseded
AD-B079172 mc

Approved for public release, distribution is unlimited

UNCLASSIFIED
SECURITY CLASSIFICATION OF THIS PAGE

AD-A168631

REPORT DOCUMENTATION PAGE

1a REPORT SECURITY CLASSIFICATION UNCLASSIFIED	1b RESTRICTIVE MARKINGS
2a SECURITY CLASSIFICATION AUTHORITY	3 DISTRIBUTION/AVAILABILITY OF REPORT
2b DECLASSIFICATION/DOWNGRADING SCHEDULE	Approved for public release; distribution is unlimited.
4 PERFORMING ORGANIZATION REPORT NUMBER(S) NOSC TR-923 Revision A	5 MONITORING ORGANIZATION REPORT NUMBER(S)
6a NAME OF PERFORMING ORGANIZATION Naval Ocean Systems Center 6b OFFICE SYMBOL (If applicable) Code 543	7a NAME OF MONITORING ORGANIZATION
6c ADDRESS (City, State and ZIP Code) San Diego, CA 92152-5000	7b ADDRESS (City, State and ZIP Code)
8a NAME OF FUNDING SPONSORING ORGANIZATION Naval Sea Systems Command 8b OFFICE SYMBOL (If applicable)	9 PROCUREMENT INSTRUMENT IDENTIFICATION NUMBER
8c ADDRESS (City, State and ZIP Code) Washington, DC 20362	10 SOURCE OF FUNDING NUMBERS PROGRAM ELEMENT NO: 62712N; PROJECT NO: SF12131691; TASK NO: NSEA; Agency Accession No.

11 TITLE (Include Security Classification)
Surface-Search Radar Performance in the Evaporation Duct: Global Predictions

12 PERSONAL AUTHOR(S)
K.D. Anderson

13a TYPE OF REPORT	13b TIME COVERED	14 DATE OF REPORT (Year, Month, Day)	15 PAGE COUNT
Final	FROM Oct 1982 TO Oct 1983	October 1983; Rev. A (May 1986)	79

16 SUPPLEMENTARY NOTATION

17 COSATI CODES			18 SUBJECT TERMS (Continue on reverse if necessary and identify by block number)
FIELD	GROUP	SUB GROUP	Surface-search radars Global predictions Free Space Selection Range (FSDR) Free Space Detection Path Loss (FSDPL)

19 ABSTRACT (Continue on reverse if necessary and identify by block number)

Surface-search radar systems, if properly designed, may utilize the oceanic surface evaporation duct to detect surface targets at ranges greater than 60 nmi. Theoretical relationships between the thickness of the evaporation duct and maximum detection range are derived for four radars at frequencies of 3, 6, 10, and 18 GHz. Distributions of maximum detection range are calculated from two worldwide duct height climatologies. The analysis considers four targets with three possible radar cross section distributions applied to each target. Since rigorous full mode waveguide analysis of all combinations is impractical, the propagation characteristics are approximated using two single mode techniques.

20 DISTRIBUTION/AVAILABILITY OF ABSTRACT	21 ABSTRACT SECURITY CLASSIFICATION
☐ UNCLASSIFIED/UNLIMITED ☒ SAME AS RPT ☐ DTIC USERS	UNCLASSIFIED
22a NAME OF RESPONSIBLE INDIVIDUAL K.D. Anderson	22b TELEPHONE (Include Area Code) (619) 225-7247 22c OFFICE SYMBOL Code 543

DD FORM 1473, 84 JAN

83 APR EDITION MAY BE USED UNTIL EXHAUSTED
ALL OTHER EDITIONS ARE OBSOLETE

UNCLASSIFIED
SECURITY CLASSIFICATION OF THIS PAGE

ACRONYMS

FSDPL	Free Space Detection Path Loss
FSDR	Free Space Detection Range
FSPL	Free Space Path Loss
MSM	Modified Single Mode
NCC	National Climatic Center
SM	Single Mode

OBJECTIVE

Currently the Navy has no reliable method to detect surface targets from a surface platform at ranges beyond the radio horizon. This report presents the global probabilities of detecting surface targets at ranges in excess of 60 nmi for various surface-search radar systems.

RESULTS

1. It is strongly believed that the most realistic description of the radar system performance is provided by the modified single mode propagation model combined with the cutoff duct height climatology. In this case, it is shown that radar system performance is influenced marginally by the target's radar cross section distribution model.

2. The average worldwide probability of detecting an average surface target at a range greater than 60 nmi for each radar is: 0.15 at 3 GHz; 0.50 at 6 GHz; 0.67 at 10 GHz; and 0.75 at 18 GHz.

3. The "best choice" radar to exploit the evaporation duct is the 18 GHz radar which is followed closely by the 10 GHz radar. Both radars perform equally well in temperate latitudes. However, in more polar latitudes, the 18 GHz radar is clearly superior.

RECOMMENDATIONS

The conclusions of this report are based on a theoretical study of propagation in the evaporation duct. Results from recent one-way path loss measurements agree reasonably well with theoretical predictions and give us confidence in the propagation models. However, these measurements are point source observations and do not account for returns from a large distributed target. Therefore, it is strongly recommended that a measurement program be initiated using a Ku-Band radar and appropriate meteorological sensors to observe and track surface targets. The objective of this program is to gather statistically significant data for validation of the propagation models.

CONTENTS

ILLUSTRATIONS

TABLES

INTRODUCTION

Currently, the Navy has no reliable method to detect surface targets from a surface platform at ranges beyond the radio horizon. In particular, there is a need to detect and target surface threats at ranges of approximately 60 nmi.

Results of recent one-way propagation measurements at 3 and 18 GHz[1] show that the oceanic evaporation duct may significantly enhance the EM field strength, especially the higher frequency, at moderate over-the-horizon ranges. For a surface target of 2.3 kiloton displacement, these measurements predict a 3 GHz radar would detect this target 30.6 percent of the time at a range of 43.7 nmi. A 18 GHz radar is predicted to detect this same target 46.8 percent of the time. These predictions assume that the surface target can be represented as a point source of large radar cross section (RCS).

In this report, we expand on the previous analytical efforts and evaluate the global probabilities of achieving detection ranges greater than 60 nmi for four radar systems against four surface targets. We analyze the results derived from two propagation models, three target RCS distribution models, and two evaporation duct height climatologies.

SURFACE TARGET DETECTION

SURFACE-SEARCH RADARS

This report considers four hypothetical, but practical, shipboard radar systems optimized for surface target detection. Table 1 lists the radar parameters. The S-Band radar is typical of existing radar systems — 2 MW radiated power, microsecond pulse width, pulse rate of 1000 pps and 32 dB antenna gain. In fact, for this radar, the only optimization made is to lower the scan rate from the typical 6 rpm to 1 rpm. This allows integration of more pulses returned from the slow moving target. As the radar frequency increases, the amount of practical transmitter power decreases. Since antenna gain becomes greater with increasing frequency, the effective radiated power is approximately the same for each of the radars.

Table 1. Radar system parameters.

RADAR NAME	S-Band	C-Band	X-Band	Ku-Band
RADAR FREQUENCY (MHz)	3000.0	6000.0	10000.0	15000.0
PEAK RADIATED POWER (kW)	2000.0	1000.0	500.0	250.0
PULSE LENGTH (usec)	1.0	1.0	1.0	1.0
PULSE RATE (pps)	1000.0	1000.0	1000.0	1000.0
NOISE FIGURE (dB)	7.0	8.0	9.0	11.0
ANTENNA GAIN (dB)	32.0	35.0	38.0	42.0
BEAM WIDTH (deg)	4.0	3.0	2.0	1.5
HORIZONTAL SCAN RATE (rpm)	1.0	1.0	1.0	1.0
ASSUMED SYSTEM LOSSES (dB)	1.0	1.5	2.0	3.0
PROBABILITY OF DETECTION	0.9	0.9	0.9	0.9
FALSE ALARM RATE	1E-8	1E-8	1E-8	1E-8
TARGET RCS (sq m)	1.0	1.0	1.0	1.0
FREE SPACE DETECTION RANGE (nmi) ..	113.2	85.9	73.5	58.2

In addition to the hardware characteristics, Table 1 lists the free space detection range (FSDR) for a point source target of 1 square metre radar cross section. The detection ranges are calculated according to the methods of Blake[2,3] for a Swirling case 1 target assuming a 0.9 probability of detection and a false alarm rate of 1.E-8.

DETECTION RANGE AND PATH LOSS

The evaluation of EM propagation (to be discussed later) is conveniently expressed in terms of path loss, the ratio of the transmitted to received power for isotropic antennas. The path loss for a system operating in free space is a function of frequency, f, and distance, d, from the transmitter. With f in MHz and d in nmi, the free space path loss (FSPL), in decibels, is

$$FSPL = 37.8 + 20\ Log(f) + 20\ Log(d)\ . \qquad (1)$$

Substituting FSDR for d in Equation 1 gives the free space detection path loss, FSDPL. This quantity permits us to relate the radar detection range to one-way path loss. For a one-way path, we can express the path loss, PL (in dB), in terms of the power transmitted, P_t, power received, P_r, transmitter gain, G_t, and receiving antenna gain, G_p, as

$$PL = P_t + G_t + G_r - P_r\ . \qquad (2)$$

FSDPL is the maximum one-way path loss allowable between the radar and the target so the radar is able to detect the target. That is, FSDPL specifies a one-way path loss threshold. If the calculated path loss is less than FSDPL, the radar is able to detect the target. Otherwise, if the path loss is greater than FSDPL, the radar cannot detect the target.

Figure 1 illustrates this concept for the S-Band radar. It is assumed that the radar antenna is 20 metres above mean sea level (msl) and the target is 10 metres above msl. The solid line of Figure 1 is the path loss predicted for standard atmospheric conditions. The dashed horizontal line corresponds to the calculated FSDPL of 149.6 dB for this radar/target combination. The

maximum detection range is where the predicted curve last intercepts the FSDPL threshold. In this case the maximum range is 16.2 nmi.

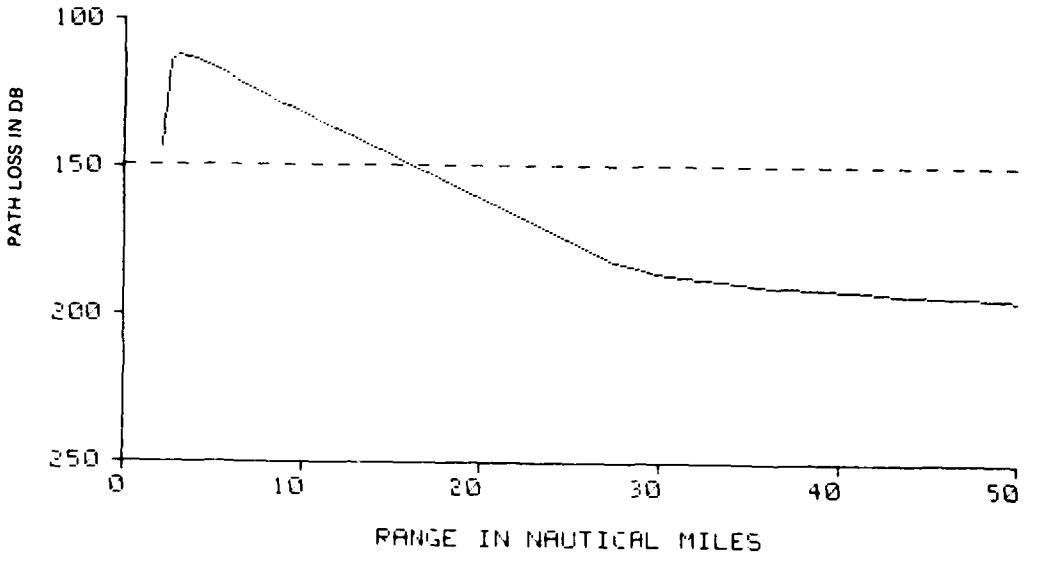

Figure 1. Path loss versus range for the S-Band radar and a target of 1 square metre RCS assuming standard atmospheric conditions. The maximum detection range is 16.2 nmi.

SURFACE TARGETS

Skolnik[4] has shown that the total RCS, σ, of typical ships is related to the radar frequency, f, and the full load displacement, D, in kilotons by the relation

$$\sigma = 52\, f^{1/2}\, D^{3/2} . \qquad (3)$$

For a surface target, σ is non-uniformly distributed with height. A model developed by Blitney[5] is assumed here and is shown in Figure 2 where the height is referenced to the target's waterline and σ is expressed as dBs above a square metre per metre of height.

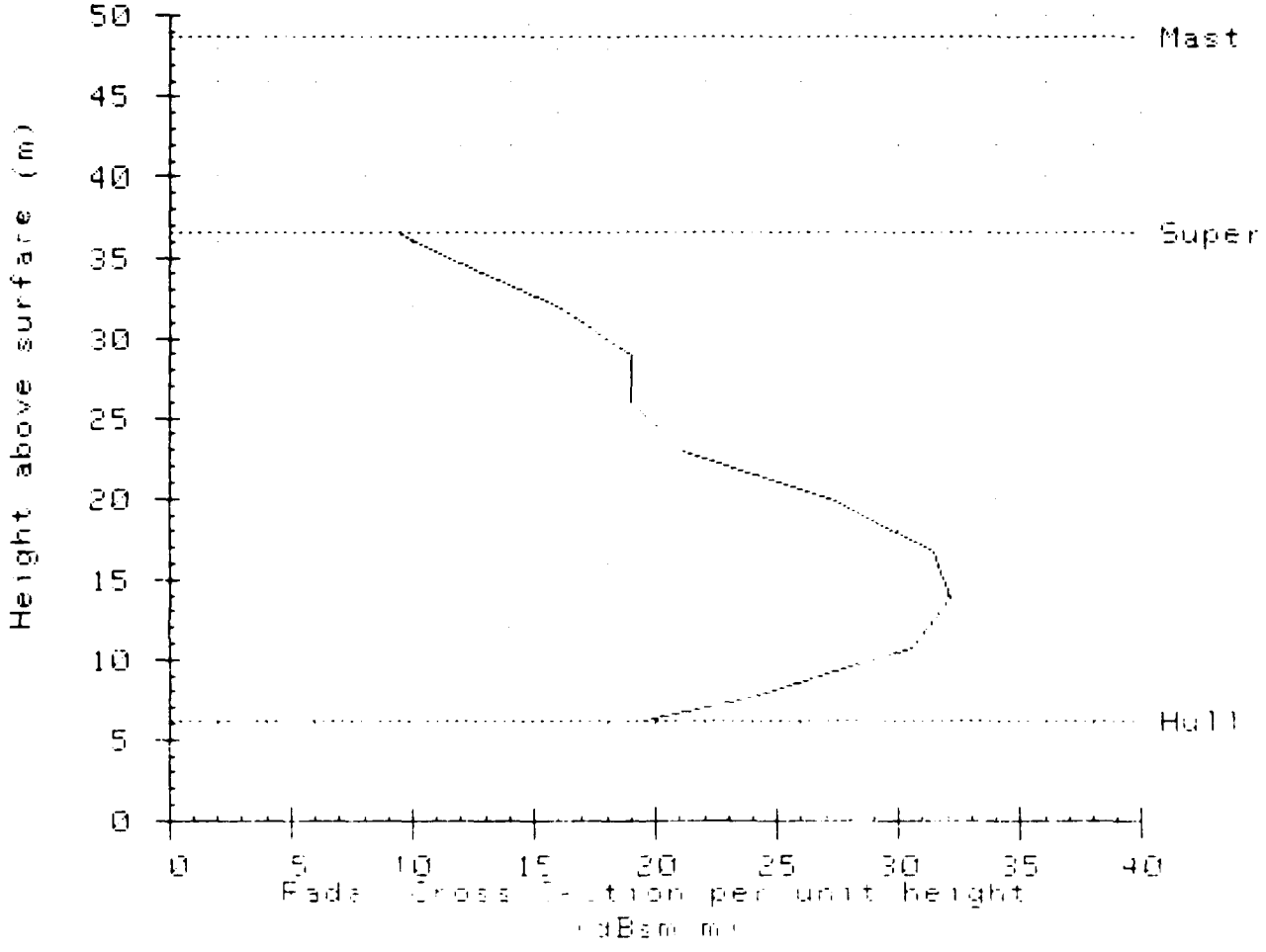

Figure 2. Conservative RCS model.

"Hull" is used to define the height region between the target's waterline and the top of the main deck. The term "Super" is used to reference the height region corresponding to the target's superstructure. The term "Mast" applies to the heights from the top of the superstructure to the topmost height of the target. These boundaries are shown by the horizontal dashed lines.

Notice that the entire σ distribution is confined to the target's superstructure region. Some RCS, rapidly decreasing above and below the superstructure, is expected but is neglected in the model. Therefore, this distribution is known as the Conservative, or C, model.

Two additional σ distribution models are analyzed. The first of these is based on the Conservative model and extrapolates σ into the height regions above and below the target's superstructure. This is known as the Extrapolated, or E, model. The third model is based on the geometric characteristics of the target where the RCS is assigned a value proportional to the area of the target. This is the geometric, or G, model. The C and the E models depend only on the target's hull, superstructure, and mast heights, whereas the G model also requires the target's silhouette.

For a distributed target, where σ_z is defined as the RCS at height z, the power received is the sum of the power returned from each height interval provided that the variation of σ_z across the interval is not too great. That is,

$$P_r = P_t \frac{G^2 \lambda^2}{(4\pi)^3 R^4} \sum F_z^4 \sigma_z \ , \tag{4}$$

where F_z is the pattern propagation factor at height z. The sum of σ_z over the target is the total RCS σ. We can replace the sum in Equation 4 by

$$\sum F_z^4 \sigma_z = \sigma \sum F_z^4 W_z \ , \tag{5}$$

where W_z is the RCS weighting factor at height z and its sum over the target's height is unity. The form of Equation 5 allows independent calculation of σ from each target description and W_z from any of the RCS models.

Three classes of surface targets are examined: cruiser (CG), destroyer (DD), and frigate (FF). One generic target is specified for the DD and FF classes and two targets are specified for the CG class. Pertinent target characteristics (displacement, heights) are given in Table 2. The CG-1 target is the most realistic target description. Tables 3 through 5 list the target's RCS weighting factors for the three distribution models. Each of the four targets is segmented into a number of one-metre thick height intervals and the weighting factor, W_z, is derived from the appropriate model. A one-metre height interval was chosen so as to minimize the height variation of σ_z over the target.

Calculating the pattern propagation factor, in terms of path loss, will be examined after a discussion of the evaporation duct.

Table 2. Surface target description.

TTRT1 Rev: 0.00

TARGET NAME	CG-1	CG-2	DD	FF
DISPLACEMENT (kton)	10.1	10.1	5.0	3.4
HEIGHT OF HULL (m)	6.0	9.0	9.0	8.0
HEIGHT OF SUPERSTRUCTURE (m)	37.0	18.0	20.0	11.0
HEIGHT OF MAST (m)	49.0	27.0	23.0	18.0
PERCENT OF AREA IN HULL	71.0	71.0	78.0	79.0
PERCENT OF AREA IN SUPERSTRUCTURE	29.0	25.0	20.0	14.0
PERCENT OF AREA IN MAST	0.0	4.0	2.0	7.0

Table 3. Target RCS weighting factors for the conservative RCS model.

Program:KTBM Rev:0.10
**** Ship RCS model: Conservative ****

Height	Radar Cross Section Weighting							
	CG-1		CG-2		DD		FF	
(m)	Target 1	HSM	Target 2	HSM	Target 3	HSM	Target 4	HSM
.5	.0000	H	.0000	H	.0000	H	.0000	H
1.5	.0000	H	.0000	H	.0000	H	.0000	H
2.5	.0000	H	.0000	H	.0000	H	.0000	H
3.5	.0000	H	.0000	H	.0000	H	.0000	H
4.5	.0000	H	.0000	H	.0000	H	.0000	H
5.5	.0000	H	.0000	H	.0000	H	.0000	H
6.5	.0151	S	.0000	H	.0000	H	.0000	H
7.5	.0151	S	.0000	H	.0000	H	.0000	H
8.5	.0151	S	.0000	H	.0000	H	.6559	S
9.5	.0634	S	.0704	S	.0424	S	.3140	S
10.5	.0688	S	.2582	S	.1788	S	.0300	S
11.5	.0688	S	.3274	S	.2631	S	.0000	M
12.5	.0933	S	.2214	S	.2511	S	.0000	M
13.5	.0995	S	.0717	S	.1524	S	.0000	M
14.5	.0995	S	.0210	S	.0586	S	.0000	M
15.5	.0891	S	.0168	S	.0189	S	.0000	M
16.5	.0847	S	.0099	S	.0137	S	.0000	M
17.5	.0847	S	.0033	S	.0123	S	.0000	M
18.5	.0541	S	.0000	M	.0063	S		
19.5	.0337	S	.0000	M	.0023	S		
20.5	.0337	S	.0000	M	.0000	M		
21.5	.0208	S	.0000	M	.0000	M		
22.5	.0079	S	.0000	M	.0000	M		
23.5	.0079	S	.0000	M				
24.5	.0067	S	.0000	M				
25.5	.0049	S	.0000	M				
26.5	.0049	S	.0000	M				
27.5	.0049	S						
28.5	.0049	S						
29.5	.0049	S						
30.5	.0044	S						
31.5	.0024	S						
32.5	.0024	S						
33.5	.0022	S						
34.5	.0008	S						
35.5	.0008	S						
36.5	.0008	S						
37.5	.0000	M						
38.5	.0000	M						
39.5	.0000	M						
40.5	.0000	M						
41.5	.0000	M						
42.5	.0000	M						
43.5	.0000	M						
44.5	.0000	M						
45.5	.0000	M						
46.5	.0000	M						
47.5	.0000	M						
48.5	.0000	M						
Sum RCS Weights	1.000		1.000		1.000		1.000	

Table 4. Target RCS weighting factors for the extrapolated RCS model.

Program:KTBM Rev:0.10
**** Ship RCS model: Extrapolated ****

Height	Radar Cross Section Weighting							
	CG-1		CG-2		DD		FF	
(m)	Target 1	HSM	Target 2	HSM	Target 3	HSM	Target 4	HSM
.5	.0003	H	.0002	H	.0002	H	.0002	H
1.5	.0003	H	.0002	H	.0002	H	.0002	H
2.5	.0003	H	.0002	H	.0002	H	.0002	H
3.5	.0022	H	.0002	H	.0002	H	.0002	H
4.5	.0022	H	.0008	H	.0008	H	.0016	H
5.5	.0022	H	.0015	H	.0015	H	.0016	H
6.5	.0149	S	.0015	H	.0015	H	.0016	H
7.5	.0149	S	.0015	H	.0015	H	.0016	H
8.5	.0149	S	.0015	H	.0015	H	.6503	S
9.5	.0629	S	.0698	S	.0421	S	.3114	S
10.5	.0682	S	.2560	S	.1773	S	.0298	S
11.5	.0682	S	.3246	S	.2608	S	.0004	M
12.5	.0926	S	.2195	S	.2490	S	.0004	M
13.5	.0986	S	.0711	S	.1511	S	.0001	M
14.5	.0986	S	.0208	S	.0581	S	.0001	M
15.5	.0884	S	.0166	S	.0187	S	.0000	M
16.5	.0840	S	.0098	S	.0136	S	.0000	M
17.5	.0840	S	.0033	S	.0122	S	.0000	M
18.5	.0536	S	.0003	M	.0062	S		
19.5	.0334	S	.0003	M	.0023	S		
20.5	.0334	S	.0002	M	.0009	M		
21.5	.0206	S	.0001	M	.0002	M		
22.5	.0078	S	.0001	M	.0000	M		
23.5	.0078	S	.0000	M				
24.5	.0066	S	.0000	M				
25.5	.0048	S	.0000	M				
26.5	.0048	S	.0000	M				
27.5	.0048	S						
28.5	.0048	S						
29.5	.0048	S						
30.5	.0043	S						
31.5	.0024	S						
32.5	.0024	S						
33.5	.0022	S						
34.5	.0008	S						
35.5	.0008	S						
36.5	.0008	S						
37.5	.0003	M						
38.5	.0003	M						
39.5	.0003	M						
40.5	.0001	M						
41.5	.0001	M						
42.5	.0001	M						
43.5	.0000	M						
44.5	.0000	M						
45.5	.0000	M						
46.5	.0000	M						
47.5	.0000	M						
48.5	.0000	M						
Sum RCS Weights	1.000		1.000		1.000		1.000	

Table 5. Target RCS weighting factors for the geometric RCS model.

Program:KTBM Rev:0.10
**** Ship RCS model: Geometric ****

Height	Radar Cross Section Weighting							
	CG-1		CG-2		DD		FF	
(m)	Target 1	HSM	Target 2	HSM	Target 3	HSM	Target 4	HSM
.5	.1183	H	.0789	H	.0867	H	.0988	H
1.5	.1183	H	.0789	H	.0867	H	.0988	H
2.5	.1183	H	.0789	H	.0867	H	.0988	H
3.5	.1183	H	.0789	H	.0867	H	.0988	H
4.5	.1183	H	.0789	H	.0867	H	.0988	H
5.5	.1183	H	.0789	H	.0867	H	.0988	H
6.5	.0094	S	.0789	H	.0867	H	.0988	H
7.5	.0094	S	.0789	H	.0867	H	.0987	H
8.5	.0094	S	.0789	H	.0867	H	.0467	S
9.5	.0094	S	.0278	S	.0182	S	.0467	S
10.5	.0094	S	.0278	S	.0182	S	.0467	S
11.5	.0094	S	.0278	S	.0182	S	.0100	M
12.5	.0094	S	.0278	S	.0182	S	.0100	M
13.5	.0094	S	.0278	S	.0182	S	.0100	M
14.5	.0094	S	.0278	S	.0182	S	.0100	M
15.5	.0094	S	.0278	S	.0182	S	.0100	M
16.5	.0094	S	.0278	S	.0182	S	.0100	M
17.5	.0094	S	.0278	S	.0182	S	.0100	M
18.5	.0094	S	.0044	M	.0182	S		
19.5	.0094	S	.0044	M	.0182	S		
20.5	.0094	S	.0044	M	.0067	M		
21.5	.0094	S	.0044	M	.0067	M		
22.5	.0094	S	.0044	M	.0067	M		
23.5	.0094	S	.0044	M				
24.5	.0094	S	.0044	M				
25.5	.0094	S	.0044	M				
26.5	.0094	S	.0044	M				
27.5	.0094	S						
28.5	.0094	S						
29.5	.0094	S						
30.5	.0094	S						
31.5	.0094	S						
32.5	.0094	S						
33.5	.0094	S						
34.5	.0094	S						
35.5	.0094	S						
36.5	.0094	S						
37.5	.0000	M						
38.5	.0000	M						
39.5	.0000	M						
40.5	.0000	M						
41.5	.0000	M						
42.5	.0000	M						
43.5	.0000	M						
44.5	.0000	M						
45.5	.0000	M						
46.5	.0000	M						
47.5	.0000	M						
48.5	.0000	M						
Sum RCS Weights	1.000		1.000		1.000		1.000	

EVAPORATION DUCTS

STABILITY

Calculation of the evaporation duct height, δ, relies on accurate measurements of the sea surface temperature and, at some reference height z_1, measurements of the air temperature, wind speed, and humidity. Details on computing δ are found in Hitney[6] and need not be repeated here. The duct height is a strong function of the air-sea temperature difference, ΔT, as shown in Figure 3. This figure illustrates the form of the δ curves parametric in relative humidity for wind speeds of 1 m/s (solid line) and 10 m/s (dotted line). In the region of thermal instability, $\Delta T < 0$, the curves are well behaved. However, near neutrality, $\Delta T = 0$, or in regions of thermal stability, $\Delta T > 0$, the curves rapidly increase. Slight errors in the measurement of ΔT can lead to significant changes in δ.

In addition, stability also influences the vertical modified refractivity profile. For example, Figure 4 shows the form of the vertical modified refractivity profile for a δ of 2.87 metres. These curves are parametric in bulk Richardson's numer, R_{1b}, which is related to ΔT by

$$R_{1b} = 369\ \Delta T/(T_a\ U^2)\ , \qquad (6)$$

where T_a is the air temperature and U is the wind speed both measured at height Z_1. Since the calculation of EM propagation parameters is highly dependent on the gradient of the M-unit profile, it is expected that stability may impact the calculations, although slightly.

WORLDWIDE DUCT HEIGHT CLIMATOLOGY

Distributions of δ have been generated by the National Climatic Center (NCC), Ashville, NC, from 10 years of shipboard surface meteorological observations. These distributions are in the form of histograms of duct height from 0 to 40 metres in increments of 2 metres. NCC processed these data in groups of Marsden Squares which are regions of the earth's surface gridded by 10° latitude and 10° longitude. A total of 212 such squares was processed

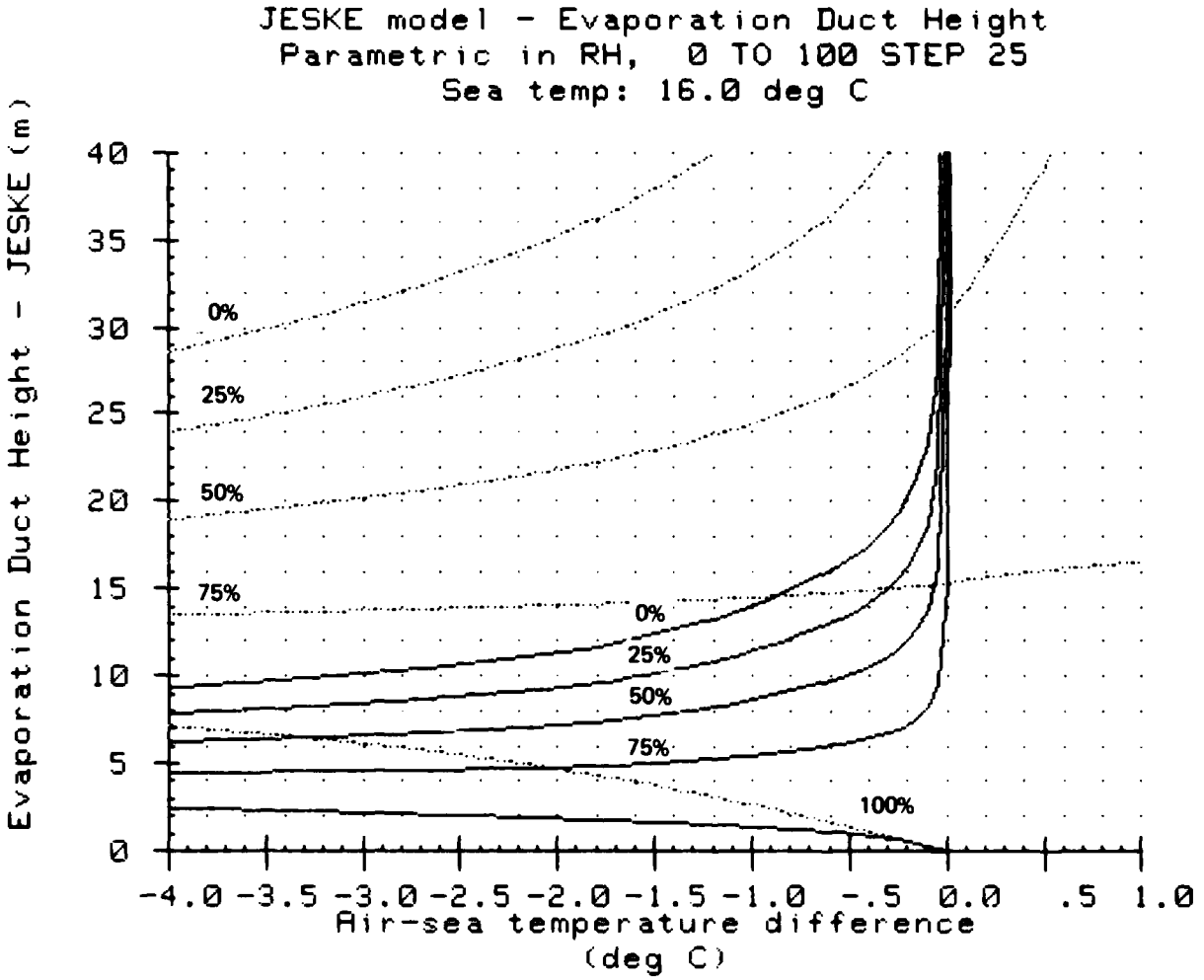

Figure 3. Evaporation duct height as a function of air-sea temperature difference, humidity, and wind speed. Solid line curves are calculated for a wind speed of 1 m/s. Dotted line curves correspond to a wind speed of 10 m/s.

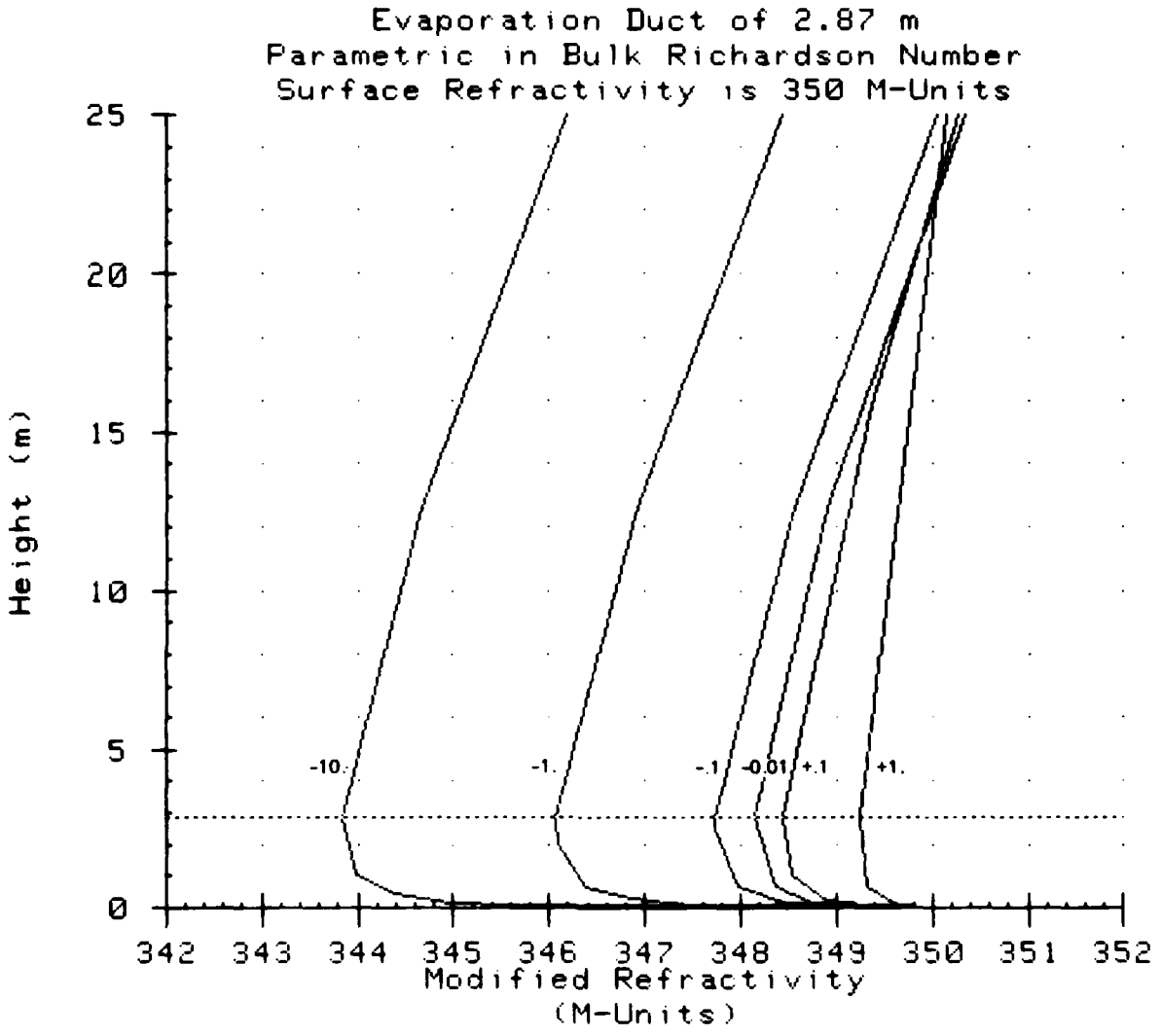

Figure 4. Vertical modified refractivity profiles for a 2.87 metre evaporation duct and the effects of thermal stability. All curves are referenced to 350 M-units at the surface.

with the δ histogram of each square independent of the other squares. The shaded regions of Figure 5 show the location of all squares contained in the climatology.

An example of the duct height histogram for the San Diego offshore area is depicted in Figure 6. The interesting feature of this figure is the high percentage of δs greater than 40 metres. It is strongly believed that these large δs are due either to measurement errors in ΔT or are caused by meteorological conditions, such as advection of continental air masses, which are not representative of the marine environment. In either case, the large values of δ are suspect. Additional support to this belief is given by experimental measurements of RF propagation in ducting environments.[1,7] These experiments show excellent agreement between theory and observations at low duct heights and considerable scatter for duct heights greater than approximately 20 metres.

EVAPORATION DUCT HEIGHT CUTOFF

As pointed out earlier, duct heights larger than 20 metres are suspect. Since the NCC duct height climatology allows these large heights, a second climatology was constructed which limits the maximum duct height to 20 metres and is known as the cutoff or limited climatology. This duct height cutoff slightly increases the percentage of time the lower duct height catagories are observed; we have reduced the total number of counts in the histogram but have not changed the number of counts in the lower histogram cells.

To keep the number of possible cross combinations in this analysis somewhat manageable, only the average day and night duct height statistics are considered. This is, the diurnal aspects of the climatology are completely ignored. In addition, all calculations are performed using the average annual statistics. Monthly data are available and could be analyzed at a later date.

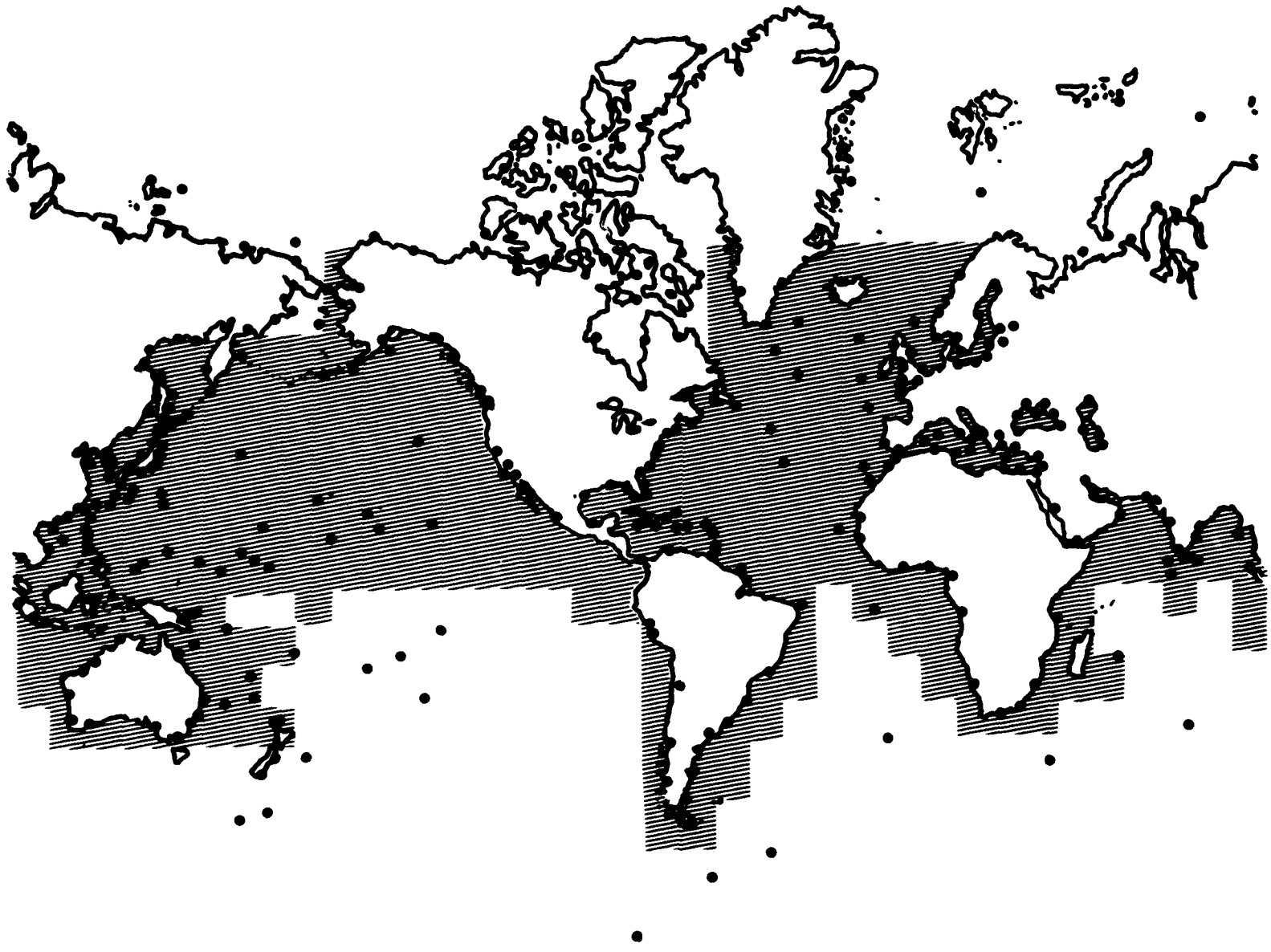

Figure 5. Geographical extent of the duct height climatology. Shaded ocean regions indicate the areas where duct height statistics are available.

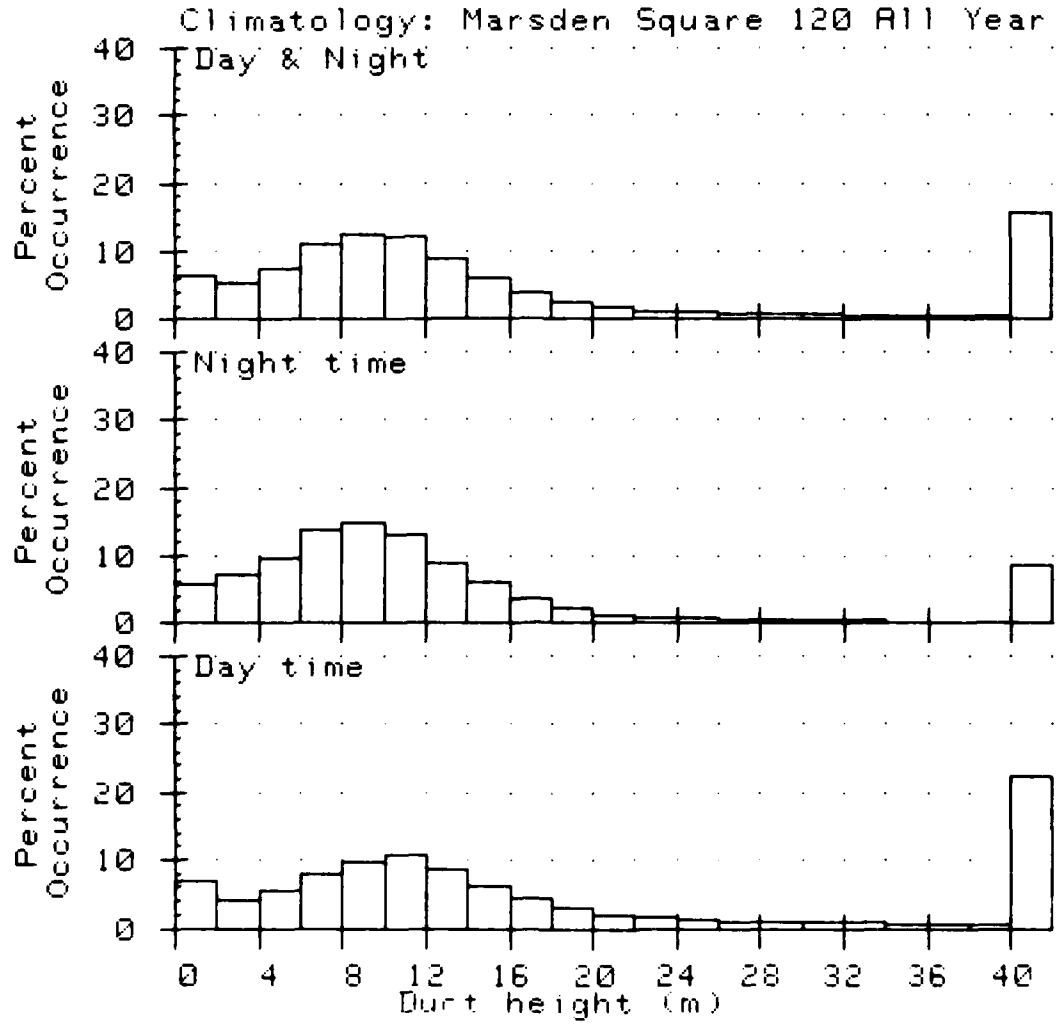

Figure 6. Duct height histogram for the San Diego offshore area (Marsden Square 120). Average yearly occurrence.

EM PROPAGATION MODELS

WAVEGUIDE TECHNIQUES

Waveguide analysis treats the EM fields as one or more discrete families, or modes, of plane waves propagating in a confined region. A number of investigators, including Pappert[8] and Hitney,[9] have used these techniques to perform detailed field calculations in tropospheric ducting environments. Results of these calculations are in agreement with experimental measurements giving a high degree of confidence in the technique.

In general, the troposphere is modeled as horizontally homogeneous, spherically symmetric layers of air. With these assumptions, the vertical height profile of the modified refractive index, M, is expressed as piecewise linear segments. Propagation parameters (phase velocities, attenuation rates) are strongly dependent on the gradient of M.

Solutions to the modal equation for realistic layered refractivity profiles are not explicit and are found through iteration techniques. A crucial problem in numerical waveguide analysis is establishing if all important modes have been found. However, no fully automated procedures have yet been developed to guarantee that all important modes are located. This uncertainty forces more hand analysis of the solutions and increases the overall cost and time.

Figure 7 presents the results of waveguide propagation analysis at 18 GHz as a function of surface evaporation duct height. The abscissa is in terms of dB path loss. As the duct thickness increases from 3 to 8 metres, the path loss decreases by 52 dB. From 8 to 11 metres, the path loss increases with increasing duct height. Further increases in duct height show that the path loss continues oscillating but (on the average) decreasing. This ringing effect is caused by competition between various modes. At 8 metres, one mode dominates. As the duct height increases, contributions from this mode decrease until, around 12 metres, a second mode becomes more effective and maximizes its contributions at 15 metres. These local path loss minimums, where a mode maximizes its influence, are assigned consecutive ordinal numbers

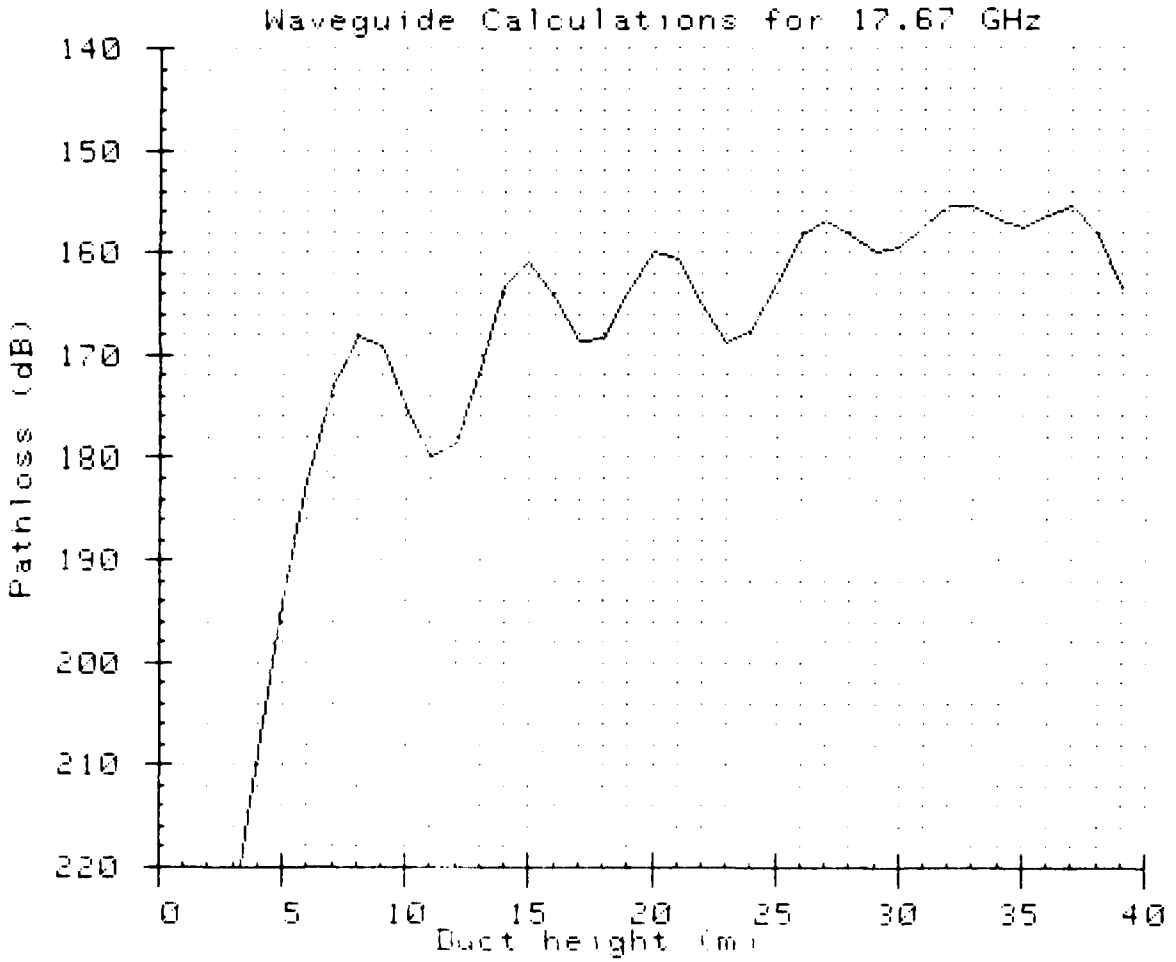

Figure 7. Path loss versus duct height at 18 GHz for a one-way 43.7 nmi path length. Full waveguide propagation analysis including 8.1 dB molecular absorption.

starting from 1. For example, mode 1 is assigned to the minimum of 8 metres, mode 2 is assigned to the minimum at 15 metres and so on.

Figure 8 is reproduced from Anderson[1] and shows the comparison of experimental measurements to the waveguide predictions at 18 GHz. For the first mode, the calculations accurately predict the minimum path loss observed, even though errors of 40 dB or more are noted. As the duct height increases, for higher modes, the agreement between the predictions and observations fails. These discrepencies are thought to arise from the assumptions of symmetry and homogeneity of the atmospheric layers. However, the important point is that the waveguide calculations, for the first mode, reasonably agree with the observation.

ABSORPTION, SCATTERING, AND SURFACE ROUGHNESS

Absorption effects in the microwave region are caused primarily by oxygen and water vapor molecules. Attenuation rates are a function of frequency and are well modeled.[10] For short path lengths, absorption may be neglected, but, for longer paths, the attenation may be noticed. In figure 8, the data were measured on an 81 km path. Width a water vapor density of 10 gm/m^3, the molecular attenuation rate is 0.1 dB/km, giving an additional loss of 8.1 dB. This loss has been accounted for in the predicted curve.

Scattering of energy by hydrometers is significant.[11] Although the attenuation may increase to several dB/km, the effects of scattering are ignored in this paper. In the surface-search radar application, the effects across the microwave frequency spectrum are comparable. That is, rain may mask a target for a radar operating at S-Band as well as for a radar operating at Ku-Band.

Small scale fluctuations in refractivity produced by turbulence may also scatter energy causing scintillation of the EM fields. It is a low elevation angle phenomena and is best modeled through probability theory. Measurements by Crane[12] and Anderson[13] provide bounds to the problem but this scattering mechanism will be ignored in the analysis.

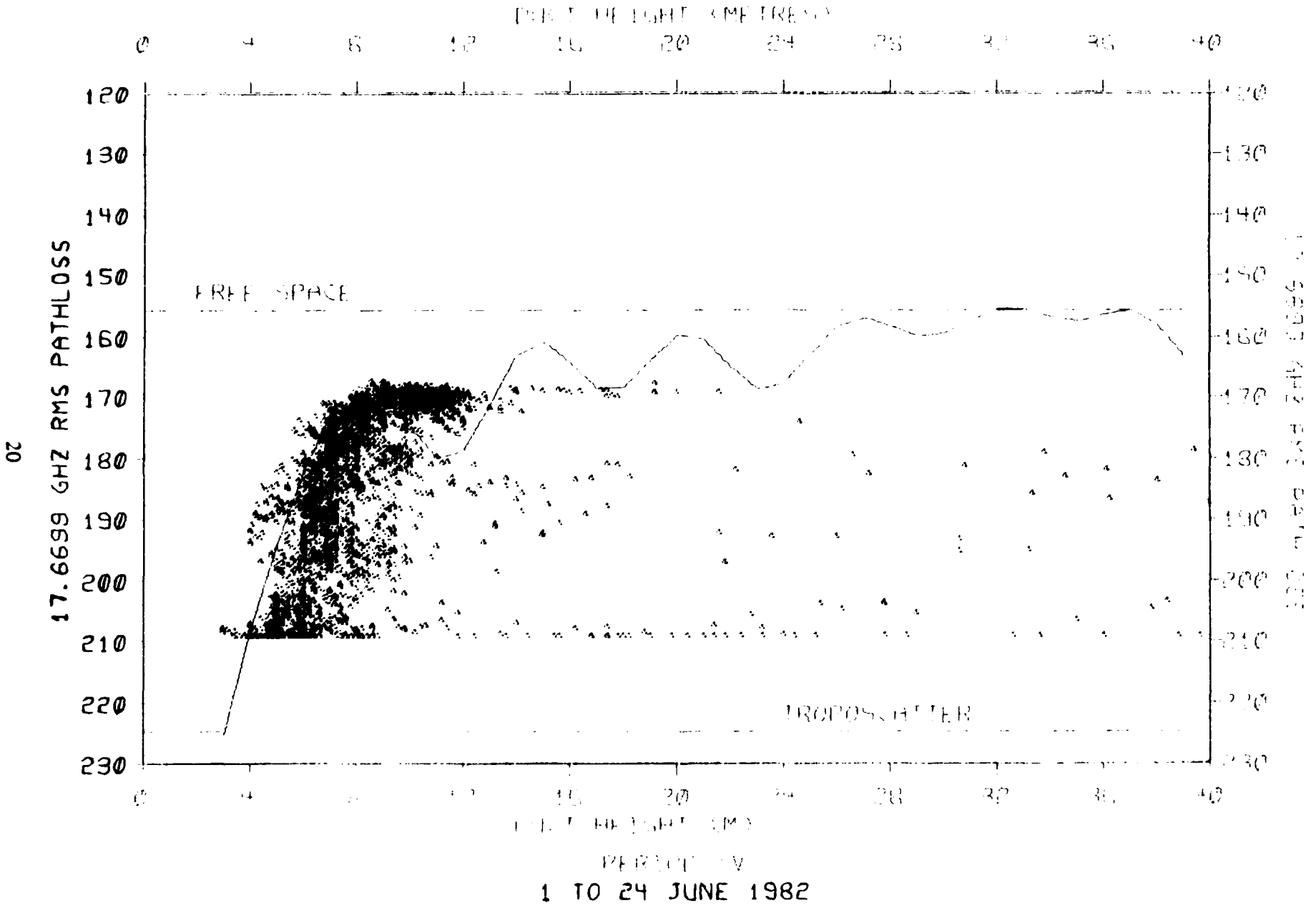
17.6699 GHZ RMS PATHLOSS
FREE SPACE
TROPOSCATTER
1 TO 24 JUNE 1982

Attenuation due to scattering from a rough surface boundary is included in the waveguide model by modifying the smooth sea reflection coefficient, R_o, with a "bump height", $\bar{h}$. That is,

$$R_g = R_o \, e^{-2(k \bar{h} \text{ sim } 4)^2} , \tag{7}$$

where $\bar{h}$ is related to the wind speed (in m/s) as

$$\bar{h} = 5.1 \times 10^{-3} U^2 . \tag{8}$$

Refer to Hitney,[6] Ament,[14] and Barrick[15] for further details. The effect of increasing $\bar{h}$ is to increase the path loss. Figure 9 shows the path loss predictions at 18 GHz for selected wind speeds or surface roughness. The solid curve is replicated from Figure 7 and is the prediction for a smooth surface. The four dotted curves correspond to the predictions for wind speeds of 2.5, 5, 7.5, and 10 m/s. In the first mode region it is observed that the highest surface roughness increases the path loss by some 7 dB. Even at this high wind speed, the contributions of surface roughness to path loss do not explain the observed differences.

WAVEGUIDE APPROXIMATIONS

To avoid the tremendous cost of full waveguide solutions required for this analysis, an approximation technique was used. This approximation method was developed by Hattan[16] who examined numerous single mode waveguide solutions at 9.6 GHz and scaled these results to other frequencies. This single mode (SM) technique accurately predicts the decrease of path loss with increasing duct height through the first mode region. However, at larger duct heights, SM results predict that the path loss increases until a "critical duct height" is reached where the path loss then remains constant. This behavior is not expected at 18 GHz since the higher order modes begin to dominate keeping the path loss low. Therefore, a modified single mode (MSM) approximation is also analyzed. MSM simply locates the minimum path loss from SM and keeps this value constant for increasing duct heights. Figure 10 shows the predictions of path loss versus duct height at 18 GHz using the full waveguide solutions

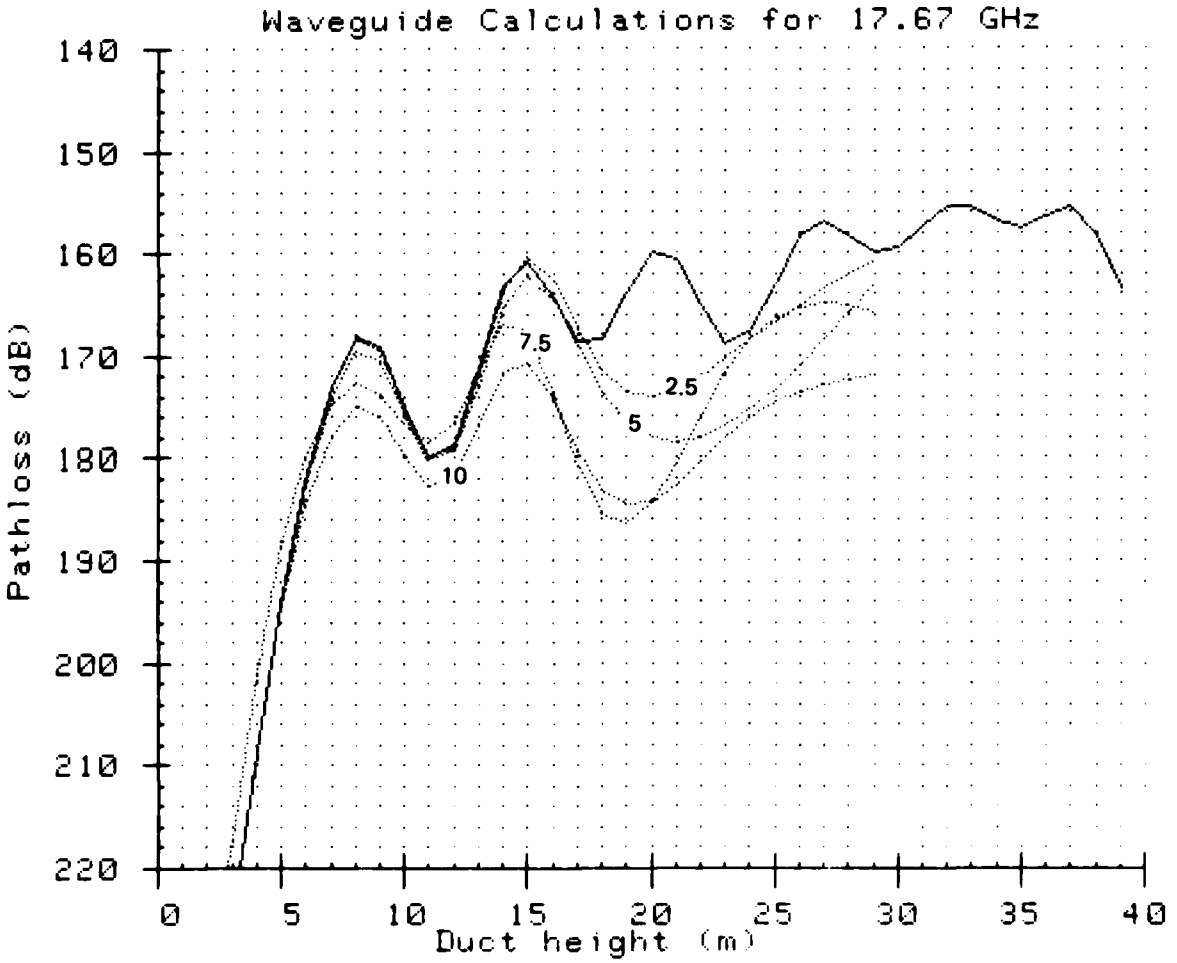

Figure 9. Effects of surface roughness. Solid line curve is the prediction for a smooth sea surface. Dotted line curves are the predictions for wind speeds of 2.5, 5, 7.5, and 10 m/s.

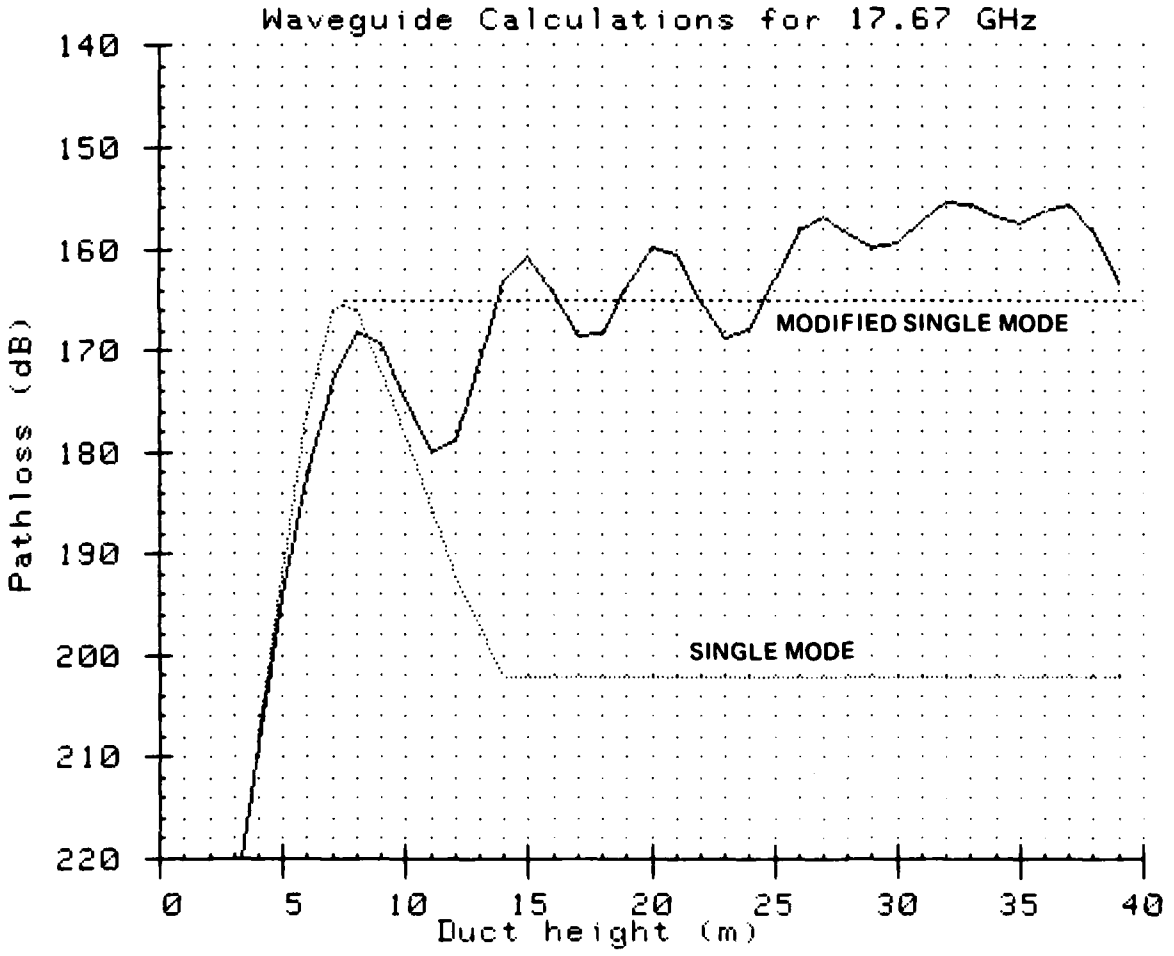

Figure 10. Path loss as a function of duct height illustrating the distinctions between the waveguide, single mode and modified single mode propagation models.

(solid line), SM approximation (dotted line) and the MSM approximation (dashed line). As seen, the MSM approximation, on the average, closely resembles the full waveguide results, whereas the SM approximation differs considerably for duct heights in excess of 15 metres.

DETECTION RANGE

Figure 11 illustrates the SM path loss predictions versus range for the S-Band radar against the CG-1 target using the C model RCS distribution. These curves are parametric in duct height which range from 0 to 40 metres in 2 metre increments. The horizontal dashed line labeled AVG is the FSDPL threshold calculated from Equation 1. Two additional thresholds are shown which represent variations in the target aspect angle. The line labeled MAX reflects the threshold for the target bow or stern on to the radar, whereas the MIN threshold is for the target broadside to the radar. In all cases, the MIN threshold is defined as AVG-8 dB and the MAX threshold is AVG+13 dB. However, we will consider only the average threshold in the following analysis.

Crosses on Figure 11 indicate the predicted detection range for the particular duct height. For example, the detection range for a δ of 20 metres intercepts the AVG threshold at a range of 81.2 nmi. Note that the path loss curves for δs of 26 metres and greater cross the AVG threshold at ranges in excess of 200 nmi. In practice, the maximum detection range is set to 200 nmi for these cases. Also note that as δ increases beyond 30 metres in height, the path loss begins to increase for increasing duct heights. This implies that the first propagation mode maximizes its influence at a δ of 30 metres for the S-Band radar.

Figure 12 presents a plot of detection range versus duct height for the same radar and target. Detection ranges, as specified by the intercept of the path loss curves with the AVG threshold, are plotted for each of the three RCS models. At 3 GHz, there is little difference between the predictions. As the radar frequency increases, the differences become pronounced. Detection range versus δ for the X-Band radar against the CG-1 target is shown in Figure 13 as an example. Similar curves are presented for all radar and target combinations in Appendix A.

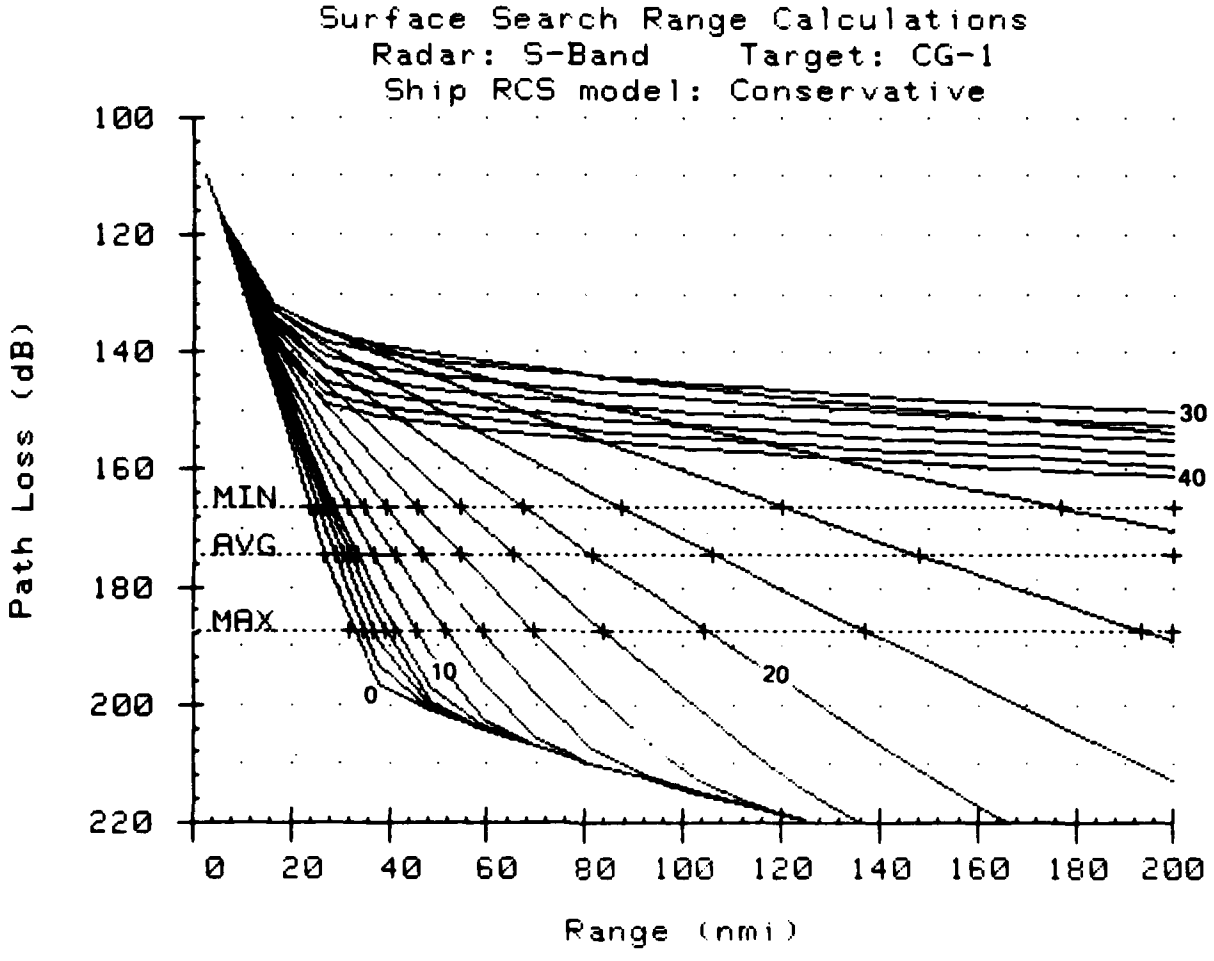

Figure 11. Path loss versus range calculated for the S-Band radar against the CG-1 target for duct heights from 0 to 40 metres.

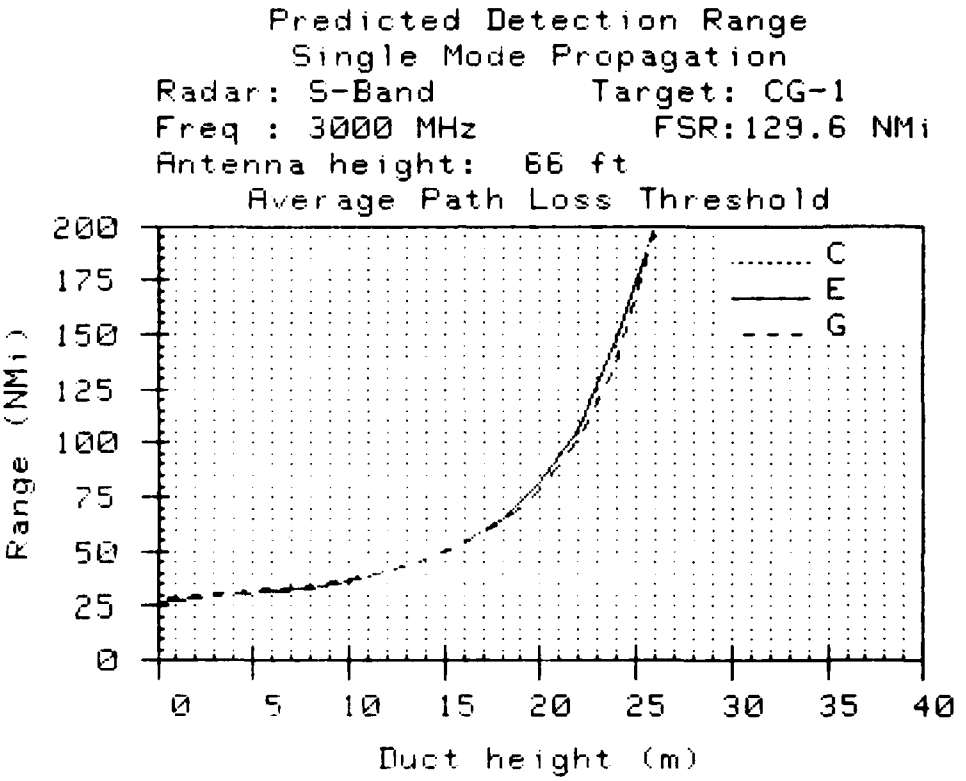

Duct Height (m)	C Model Range (NMi)	E Model Range (NMi)	G Model Range (NMi)
0.0	26.7	26.8	27.6
2.0	28.9	29.0	29.8
4.0	30.6	30.7	31.5
6.0	32.0	32.1	33.0
8.0	33.5	33.5	34.3
10.0	36.7	36.7	37.3
12.0	41.0	41.1	41.4
14.0	46.8	46.8	46.7
16.0	54.6	54.6	54.0
18.0	65.4	65.4	64.1
20.0	81.2	81.2	78.8
22.0	105.9	105.9	102.0
24.0	147.7	147.7	137.3
26.0	200.0	200.0	200.0
28.0	200.0	200.0	200.0
30.0	200.0	200.0	200.0
32.0	200.0	200.0	200.0
34.0	200.0	200.0	200.0
36.0	200.0	200.0	200.0
38.0	200.0	200.0	200.0
40.0	200.0	200.0	200.0

Figure 12. Maximum detection range for a standard surface duct as a function of duct height and RCS model.

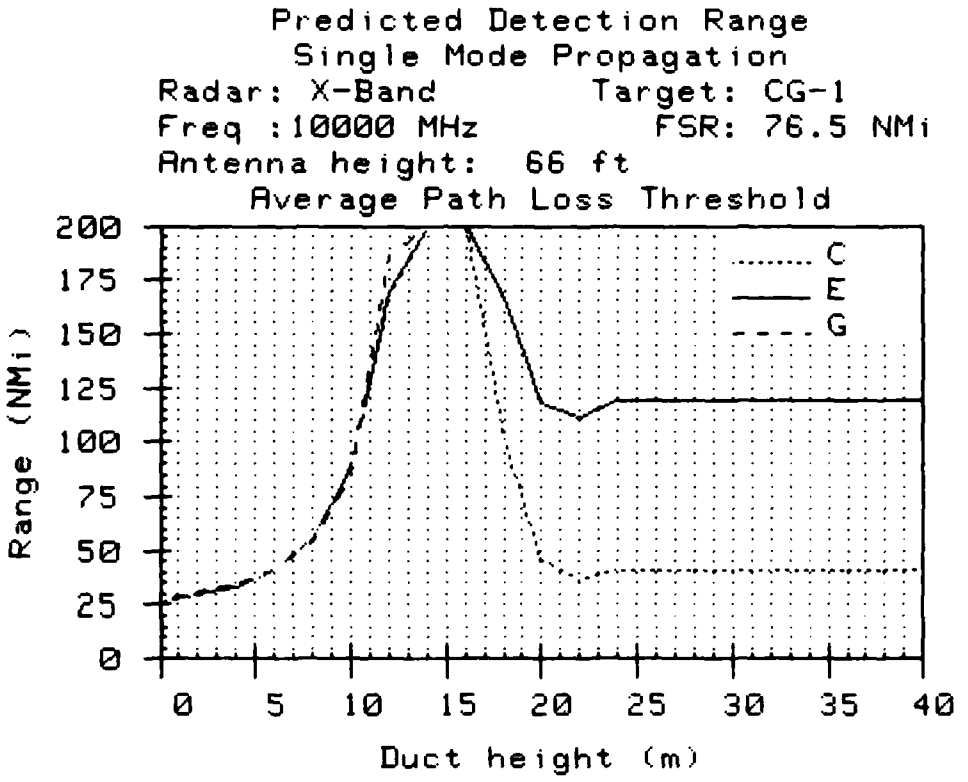

Duct Height (m)	C Model Range (NMi)	E Model Range (NMi)	G Model Range (NMi)
0.0	26.3	26.5	27.2
2.0	30.4	30.5	31.3
4.0	33.4	33.5	34.2
6.0	41.0	41.0	41.2
8.0	55.5	55.5	54.4
10.0	88.6	88.5	85.5
12.0	169.2	169.9	186.7
14.0	200.0	200.0	200.0
16.0	200.0	200.0	200.0
18.0	100.8	166.8	200.0
20.0	46.0	118.1	200.0
22.0	36.2	111.7	200.0
24.0	41.1	119.6	200.0
26.0	41.1	119.6	200.0
28.0	41.1	119.6	200.0
30.0	41.1	119.6	200.0
32.0	41.1	119.6	200.0
34.0	41.1	119.6	200.0
36.0	41.1	119.6	200.0
38.0	41.1	119.6	200.0
40.0	41.1	119.6	200.0

Figure 13. Maximum detection range versus duct height for the X-Band radar showing the differences predicted between the RCS models.

GLOBAL RADAR SYSTEM PERFORMANCE

PERCENT OCCURRENCE

Once the form of the detection range versus duct height is established, the duct height climatology may be used to determine the percentage of time the detection range exceeds a specified range. In this analysis, we have chosen to examine the percentage of time the detection range is greater than 60 nmi. Considering that the radar antennas are all 20 metres above msl, this range is 2.4 times the normal horizon range for the radars against the CG-1 target and 3.2 times the horizon range for the FF target. The determination of the percentage of time the detection range exceeds 60 nmi from the δ climatology is simply the sum of the percentage of occurrence of duct heights observed where the detection range is predicted to exceed the specified range. For example, from Figure 12, the detection range is greater than 60 nmi for δs greater than 15 metres. At the higher radar frequencies, the propagation models (SM or MSM) and the RCS models (C, E, or G) have considerable influence. From Figure 13, the X-Band radar, using the conservative RCS model for the CG-1 target and the SM propagation model, is predicted to achieve detection ranges in excess of 60 nmi for duct heights in the interval of 8.3 to 19.5 metres. With the MSM propagation model, the X-Band radar is predicted to exceed 60 nmi detection ranges against the CG-1 target from all duct heights greater than 8.3 metres.

We consider three RCS models, two propagation models, four radars, four targets, two duct height climatologies and 212 Marsden Squares giving a total of 40,704 possible combinations. To provide a reasonable presentation of the results, we will examine in the following sections the average global probabilities by propagation model, climatology, and RCS model.

SINGLE MODE PREDICTIONS

NCC Climatology

Table 6 presents the worldwide average percentage of time that the radars are expected to detect the targets at ranges greater than 60 nmi. Note that

the S-Band radar is predicted to observe the CG-1 target approximately 41 percent of the time. This hypothetical radar is very close in performance characteristics to existing operational radars and these radars are known not to observe targets as frequently as predicted. The high percentage for the S-Band radar is brought about from allowing large duct heights in the climatology as will be illustrated in the next section.

Table 6. Percent occurrence of detection ranges greater than 60 nmi: Single mode, NCC climatology.

	Conservative RCS				Extrapolated RCS				Geometric RCS			
Target	S	C	X	Ku	S	C	X	Ku	S	C	X	Ku
CG-1	41.7	64.6	41.6	12.5	41.7	64.6	74.9	16.6	41.0	64.0	74.6	81.0
CG-2	40.5	64.0	36.0	12.4	40.5	64.0	74.7	14.1	39.6	63.4	74.5	80.9
DD	38.6	43.8	33.7	9.0	38.6	62.9	42.3	11.4	37.4	61.9	73.9	80.5
FF	36.7	61.4	35.6	10.3	36.7	61.4	41.4	11.5	35.9	60.9	73.4	80.2

The effects of the RCS models are noted for the higher frequency radars. The G model predicts that the Ku-Band radar detects CG-1 81 percent of the time, whereas the C and E models predict approximately 17 percent. This is expected as the G model has the highest concentration of RCS in the target's hull region.

Cutoff Climatology

Table 7 lists the percentages calculated for the duct height distribution where the maximum duct height is limited to 20 metres. The predictions for the S-Band radar against the CG-1 target have dropped from the previous 41 percent to 16 percent. This lower percentage is more in line with Fleet experience.

Table 7. Percent occurrence of detection ranges greater than 60 nmi: Single mode, Cutoff climatology.

	Conservative RCS				Extrapolated RCS				Geometric RCS			
Target	S	C	X	Ku	S	C	X	Ku	S	C	X	Ku
CG-1	16.8	52.9	65.0	17.3	16.8	52.9	67.7	23.5	15.6	52.0	67.3	76.0
CG-2	14.8	52.1	65.6	17.2	14.8	52.1	67.5	19.8	13.3	51.2	67.1	75.9
DD	11.6	50.4	52.0	12.4	11.6	50.4	66.4	15.8	9.7	48.9	66.3	75.3
FF	8.4	48.2	55.2	14.3	8.4	48.2	65.0	15.9	7.1	47.5	65.6	74.9

Notice that the percentages predicted for both the S and C-Band radars are generally lower than the predictions using the NCC climatology. The cutoff climatology predictions for the X and Ku-Band radars are higher than the NCC predictions using the C model and are lower using the G model. With the E model, the X-Band percentages are mixed and the Ku-Band radar percentages are higher. This indicates a very complex relationship between the RCS model and the duct height distributions that is not fully understood yet.

MODIFIED SINGLE MODE PREDICTIONS

NCC Climatology

Table 8 lists the percentages found using the MSM propagation model and the NCC climatology. The percentages for the S and C-Band radars are nearly identical to the SM predictions above. Again, the predictions for the S-Band radar are much higher than observed within the Fleet. The G model predictions for the X and Ku-Band radars are identical to the SM results. C and E model predictions for the X-Band radar are higher than the SM predictions and the Ku-Band radar percentages dramatically jump from 15 percent to 80 percent. This is expected as the MSM model does not allow the detection range to decrease with increasing duct heights.

Table 8. Percent occurrence of detection ranges greater than 60 nmi: Modified single mode, NCC climatology.

	Conservative RCS				Extrapolated RCS				Geometric RCS			
Target	S	C	X	Ku	S	C	X	Ku	S	C	X	Ku
CG-1	41.7	64.6	74.9	80.6	41.7	64.6	74.9	80.6	41.0	64.0	74.6	81.0
CG-2	40.5	64.0	74.7	80.6	40.5	64.0	74.7	80.6	39.6	63.4	74.5	80.9
DD	38.6	62.9	74.2	79.8	38.6	62.9	74.2	79.9	37.4	61.9	73.9	80.5
FF	36.7	61.4	73.8	79.7	36.7	61.4	73.8	79.7	35.9	60.9	73.4	80.2

Cutoff Climatology

Table 9 lists the percentages calculated for the MSM propagation model using the limited climatology. The percentages found for a particular radar are only slightly changed between the three RCS models. The Ku-Band radar shows the highest probability of detecting a target. In general, the S-Band

radar is expected to detect a surface target at a range greater than 60 nmi approximately 15 percent of the time: C-Band radar, 52 percent; X-Band radar, 67 percent; and the Ku-Band radar, 75 percent.

Table 9. Percent occurrence of detection ranges greater than 60 nmi: Modified single mode, Cutoff climatology.

	Conservative RCS				Extrapolated RCS				Geometric RCS			
Target	S	C	X	Ku	S	C	X	Ku	S	C	X	Ku
CG-1	16.8	52.9	67.7	75.4	16.8	52.9	67.7	75.5	15.6	52.0	67.3	76.0
CG-2	14.8	52.1	67.5	75.4	14.8	52.1	67.5	75.4	13.3	51.2	67.1	75.9
DD	11.6	50.4	66.8	74.4	11.6	50.4	66.8	74.4	9.7	48.9	66.3	75.3
FF	8.4	48.2	66.1	74.2	8.4	48.2	66.1	74.2	7.1	47.5	65.6	74.9

DETAILED EXAMINATION OF GLOBAL PROBABILITIES

From the previous discussions, it is thought that the predictions for MSM propagation combined with the cutoff climatology are the best estimates of system performance. Since the conservative RCS model and the CG-1 target are the most realistic target descriptions, the predictions will be closely examined.

Figures 14 through 17 are world map plots of percentage occurrence of detection ranges in excess of 60 nmi for the four radar systems. The percent occurrence derived from the duct height distribution for each of the Marsden Squares in the climatology is plotted at the squares' geographic location. The legend describing the color assigned to 10 percent intervals of occurrence is shown by the color bars on the left hand side of each plot. Zero to 9.9 percent occurrence is plotted as light yellow, 10 to 19.9 percent occurrence is plotted as a darker yellow and so on. From these figures, it is apparent that the evaporation duct strongly affects the propagation characteristics in the temperate latitudes and is somewhat weaker in the more polar latitudes. Even though the S-Band radar detects the target only 16.8 percent of the time on the (global) average, at 15° north latitude the occurrence is 27.7 percent. However, at 65° north latitude, the percentage drops to 1.4 percent. At 15° north latitude the occurrence for the other radars is C-Band, 73.1 percent; X-Band, 85 percent; and Ku-Band, 89.7 percent. At 65° north latitude the percentages are: C-Band, 10.4 percent; X-Band, 27.2 percent; and Ku-Band, 42.4

percent. The figures in Appendix B list the occurrence percentage for each radar and target combination by individual Marsden Square.

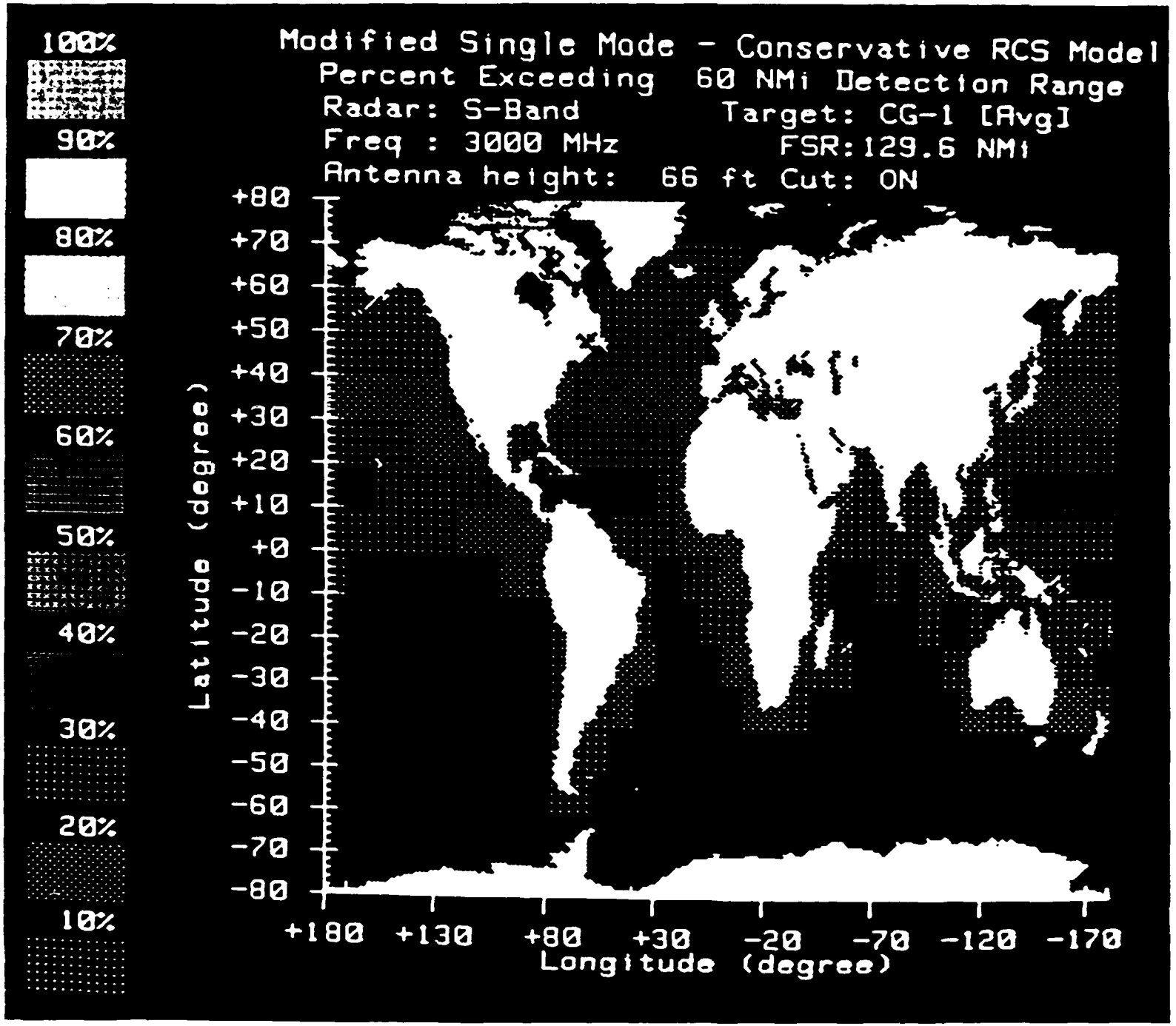

Figure 1-4 Percent occurrence of detection ranges greater than 60 nmi for the S-Band radar

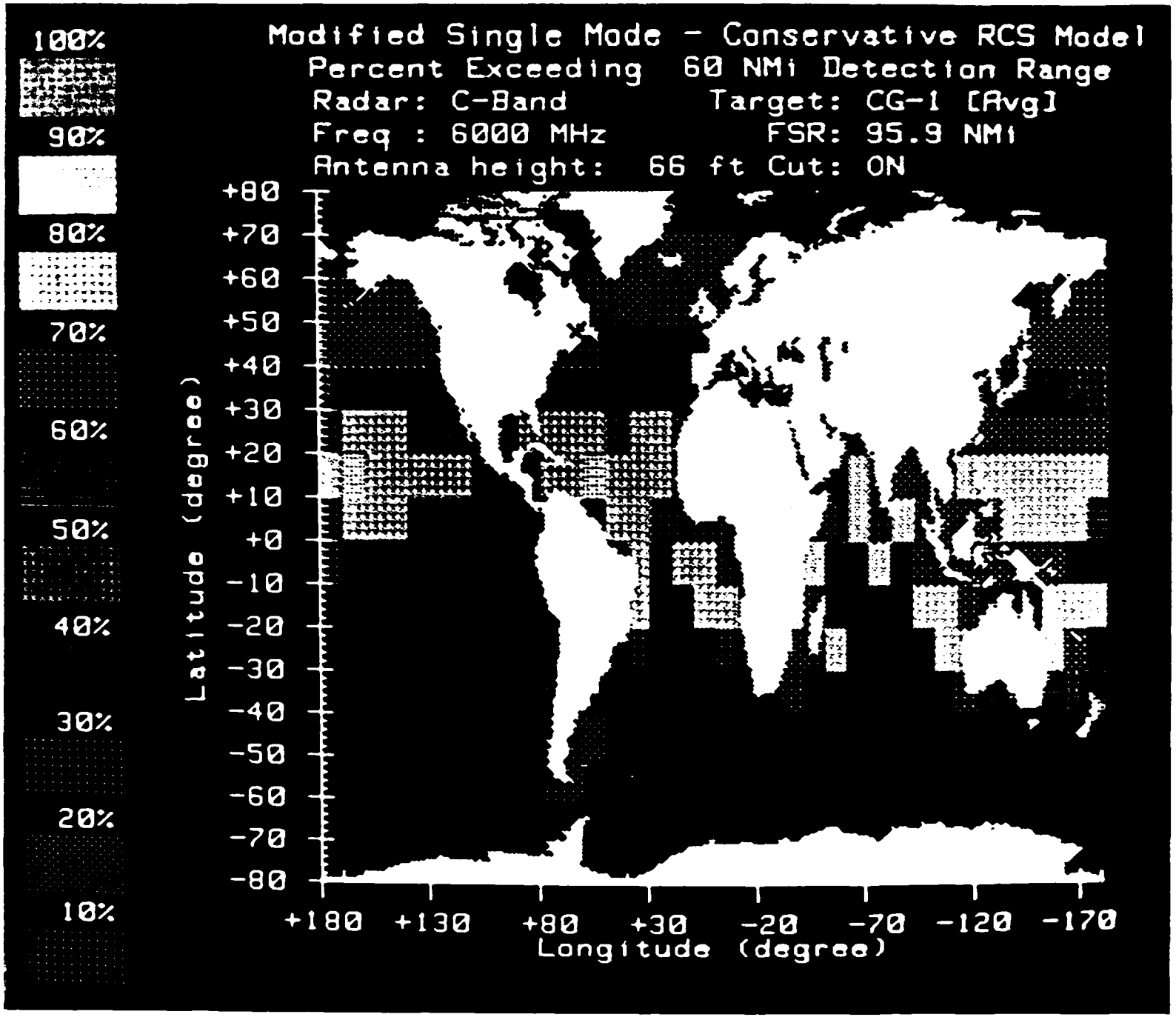

Figure 15 Percent occurrence of detection ranges greater than 60 nmi for the C-Band radar

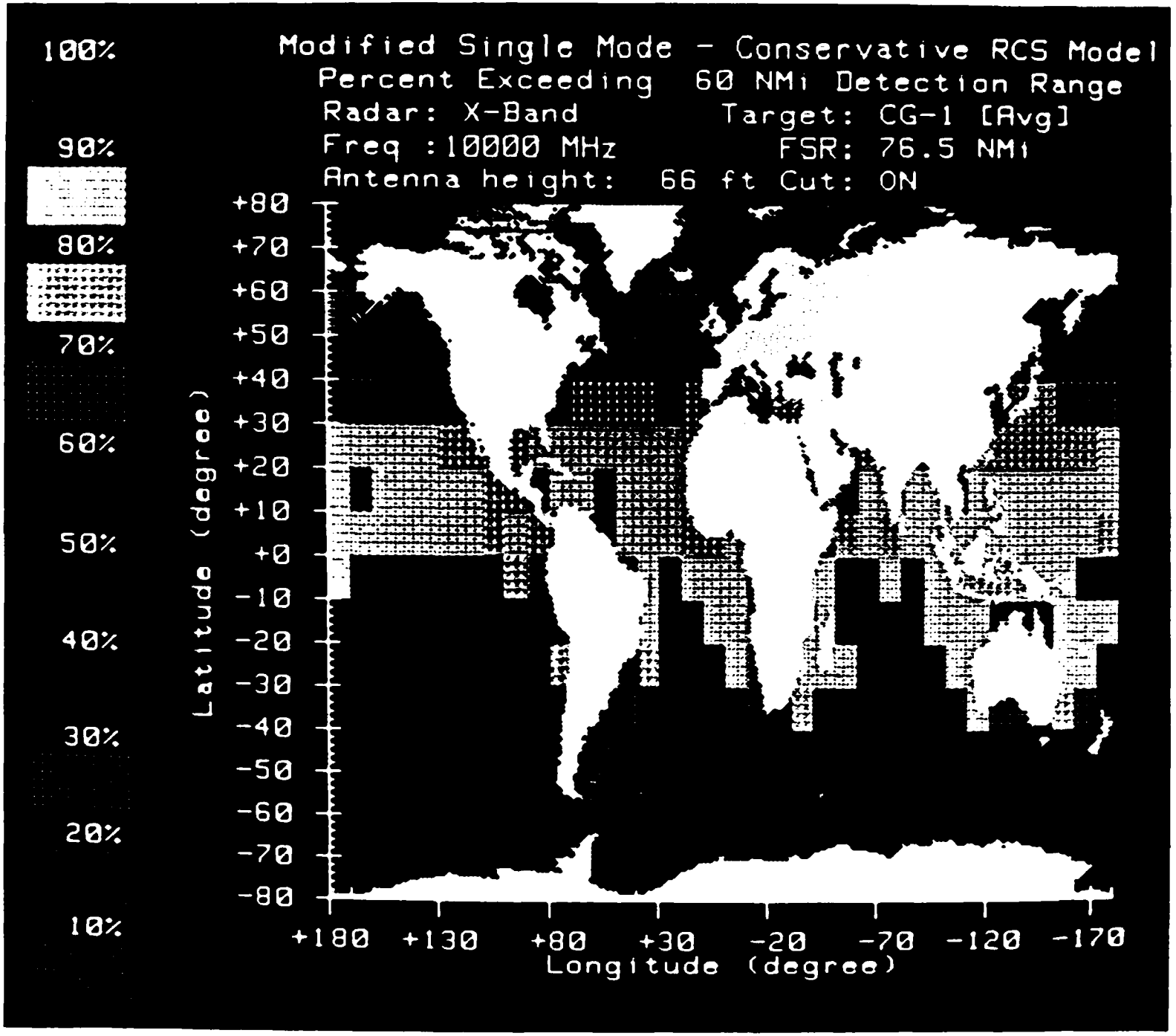

Figure 16 Percent occurrence of detection ranges greater than 60 nmi for the X-Band radar.

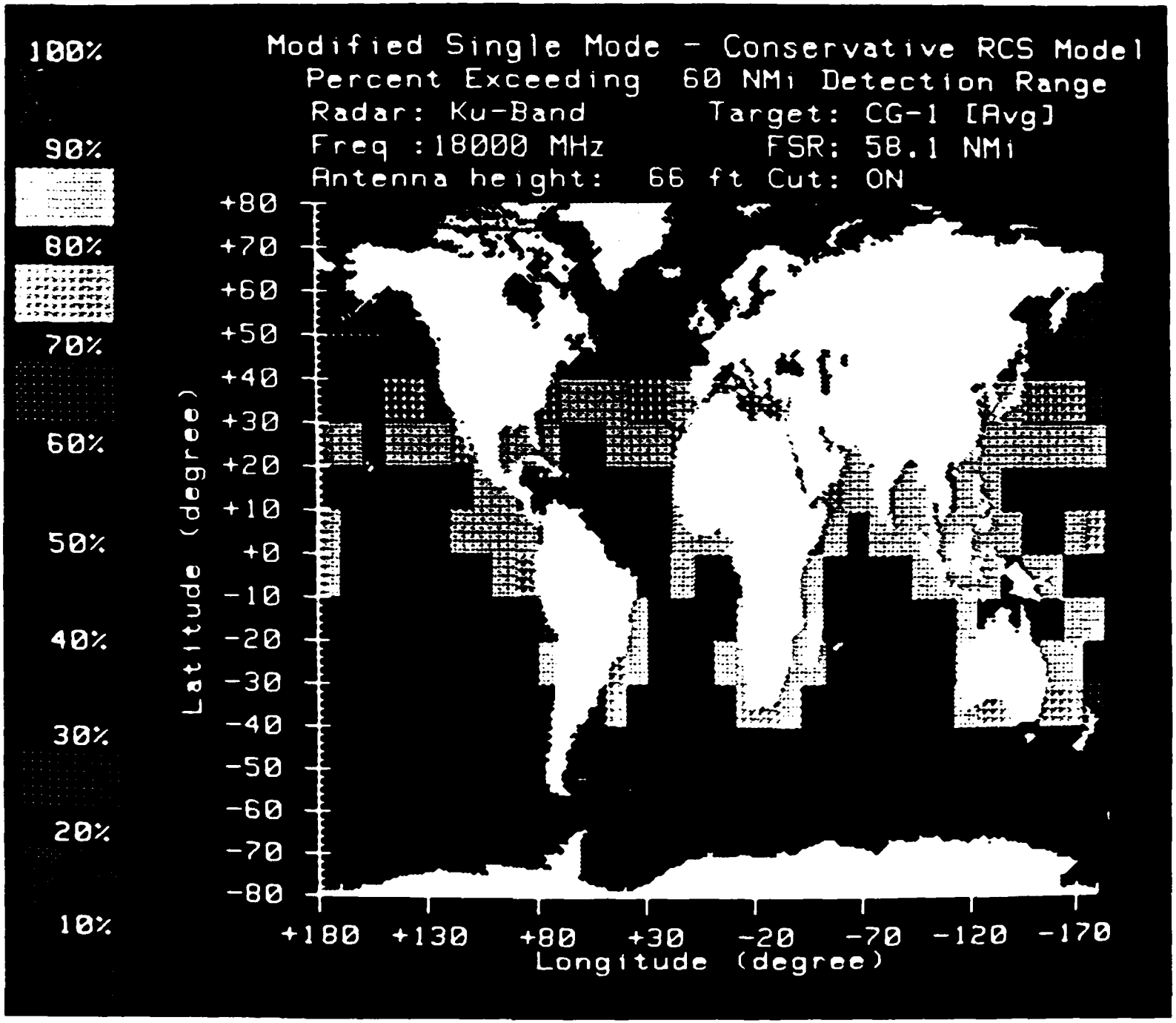

Figure 17. Percent occurrence of detection ranges greater than 60 nmi for the Ku-Band radar.

CONCLUSIONS

Predictions indicate that the Ku-Band radar is the "best" radar to use for surface target detection at ranges in excess of 60 nmi. In temperate latitudes, it is expected that this radar can achieve these detection ranges nearly 90 percent of the time. At higher latitudes, the percentage falls off to approximately 40 percent. However, a detection probability of 0.4 is significant considering current surface-search radar capabilities at these ranges.

It is important to note that the surface oceanic evaporation duct allows the long range detection. This atmospheric ducting phenomena is exploitable and considerable advantage may be gained by properly designing surface-search radar systems to make full use of the propagation enhancements available.

REFERENCES

1. Anderson, K.D., Evaporation Duct Effects on Moderate Range Propagation Over the Sea at 10 and 1.7 cm Wavelengths, Naval Ocean Systems Center TR 858, 19 November 1982.
2. Blake, L.V., A FORTRAN Computer Program to Calculate the Range of a Pulse Radar, Naval Research Laboratory Report 7448, 28 August 1972.
3. Blake, L.V., A Guide to Basic Pulse Radar Maximum-Radar Calculation Part 1, Naval Research Laboratory Report 6930, 23 December 1969.
4. Skolnik, M.I., An Empirical Formula for the Radar Cross Section of Ships at Grazing Incidence, IEEE Trans of Aero. and Elec. Systems, March 1974, p 292.
5. Hitney, H.V., Private communication.
6. Hitney, H.V., Propagation Modeling in the Evaporation Duct, Naval Electronics Laboratory Center TR 1947, 1 April 1975.
7. Jeske, H., Die Ausbreitung Elektromagnetischer Wellen im cum-bis m-Band Uber dem Meer unter besonderer Berucksichtigung der meterologischen Bedingungen in der Maritimen Grenzschicht, Hamburger Geophysikalische Einzelschriften, 1965, De Gruyter and Co., Hamburg.
8. Pappert, R.A., and C.L. Goodhart, Case Studies of Beyond-the-Horizon Propagation in Tropospheric Ducting Environments, Radio Sci., 12, 1977, pp 75-87.
9. Hitney, H.V., et al, Evaporation Duct Influences on Beyond-the-Horizon High Altitude Signals, Radio Sci., 13, 1978, pp 559-675.
10. Liebe, H.J., Modeling Attenuation and Phase of Radio Waves in Air at Frequencies Below 1000 GHz, Radio Sci., 6, 1981, pp 1183-1199.
11. Crane, R.K., Fundamental Limitations Caused by RF Propagation, Proc. IEEE, 69, 1981, pp 196-209.
12. Crane, R.K., Analysis of Tropospheric Effects at Low Elevation Angles, Rome Air Development Center TR 78-252, 1978.
13. Anderson, K.D., Inference of Refractivity Profiles by Satellite-to-Ground RF Measurements, Radio Sci., 3, 1982, pp 653-663.
14. Ament, W.S., Toward a Theory of Reflection by a Rough Surface, Proc. IRE, 41, 1953, pp 142-146.

15. Barrick, D.E., Theory of HF and VHF Propagation Across the Rough Sea, 1, The Effective Surface Impedence for a Slightly Rough Highly Conductive Medium at Grazing Incidence, Radio Sci., 6, 1971, pp 517-526.

16. Hattan, C.P., Propagation Models for IREPS Revision 2.0, Naval Ocean Systems Center TR 771, 28 April 1982.

APPENDIX A

Maximum detection range versus evaporation duct height for all combinations of the four radar systems with the four targets are shown in Figures A1 through A16.

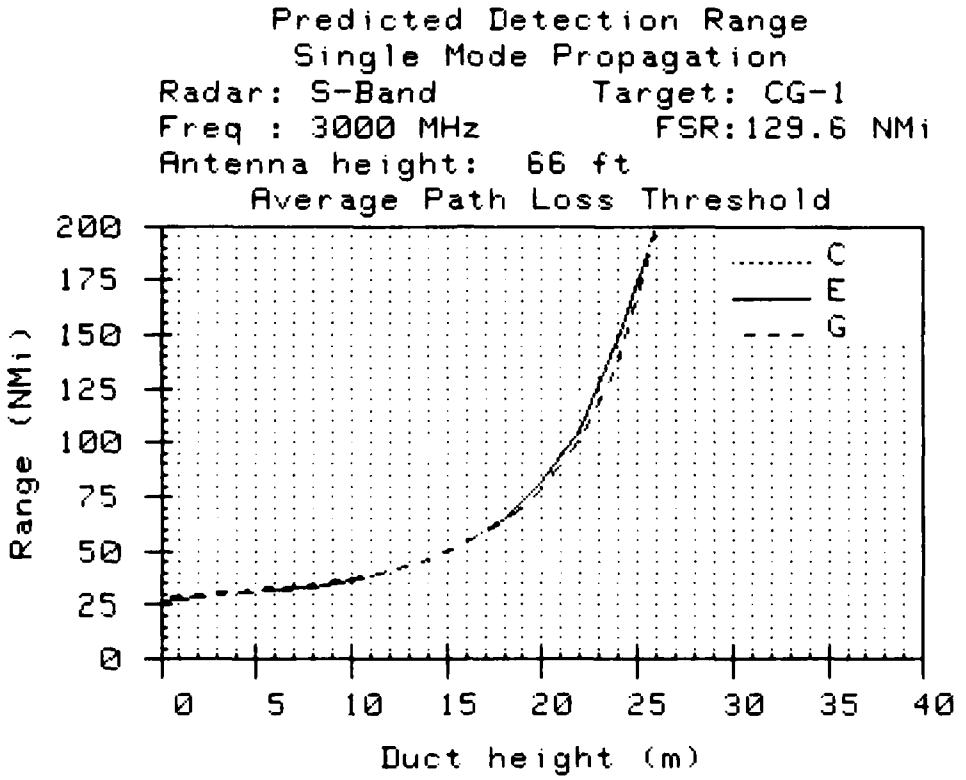

Duct Height (m)	C Model Range (NMi)	E Model Range (NMi)	G Model Range (NMi)
0.0	26.7	26.8	27.6
2.0	28.9	29.0	29.8
4.0	30.6	30.7	31.5
6.0	32.0	32.1	33.0
8.0	33.5	33.5	34.3
10.0	36.7	36.7	37.3
12.0	41.0	41.1	41.4
14.0	46.8	46.8	46.7
16.0	54.6	54.6	54.0
18.0	65.4	65.4	64.1
20.0	81.2	81.2	78.8
22.0	105.9	105.9	102.0
24.0	147.7	147.7	137.3
26.0	200.0	200.0	200.0
28.0	200.0	200.0	200.0
30.0	200.0	200.0	200.0
32.0	200.0	200.0	200.0
34.0	200.0	200.0	200.0
36.0	200.0	200.0	200.0
38.0	200.0	200.0	200.0
40.0	200.0	200.0	200.0

Figure A1

Program: MRtplt Rev:0.00

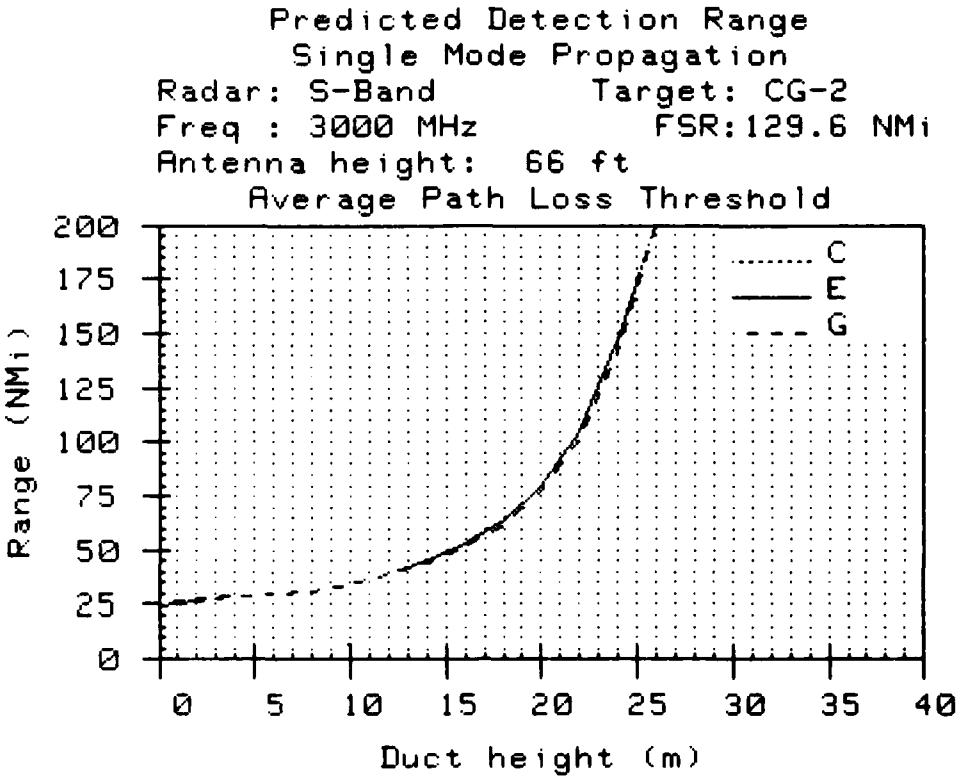

Duct Height (m)	C Model Range (NMi)	E Model Range (NMi)	G Model Range (NMi)
0.0	24.5	24.5	25.2
2.0	26.7	26.7	27.2
4.0	28.4	28.4	28.9
6.0	29.8	29.8	30.2
8.0	31.3	31.3	31.6
10.0	34.5	34.5	34.6
12.0	39.0	39.0	38.8
14.0	44.8	44.8	44.3
16.0	52.7	52.7	51.8
18.0	63.7	63.7	62.3
20.0	79.6	79.6	77.6
22.0	104.5	104.5	101.5
24.0	147.1	147.0	141.2
26.0	200.0	200.0	200.0
28.0	200.0	200.0	200.0
30.0	200.0	200.0	200.0
32.0	200.0	200.0	200.0
34.0	200.0	200.0	200.0
36.0	200.0	200.0	200.0
38.0	200.0	200.0	200.0
40.0	200.0	200.0	200.0

Figure A2

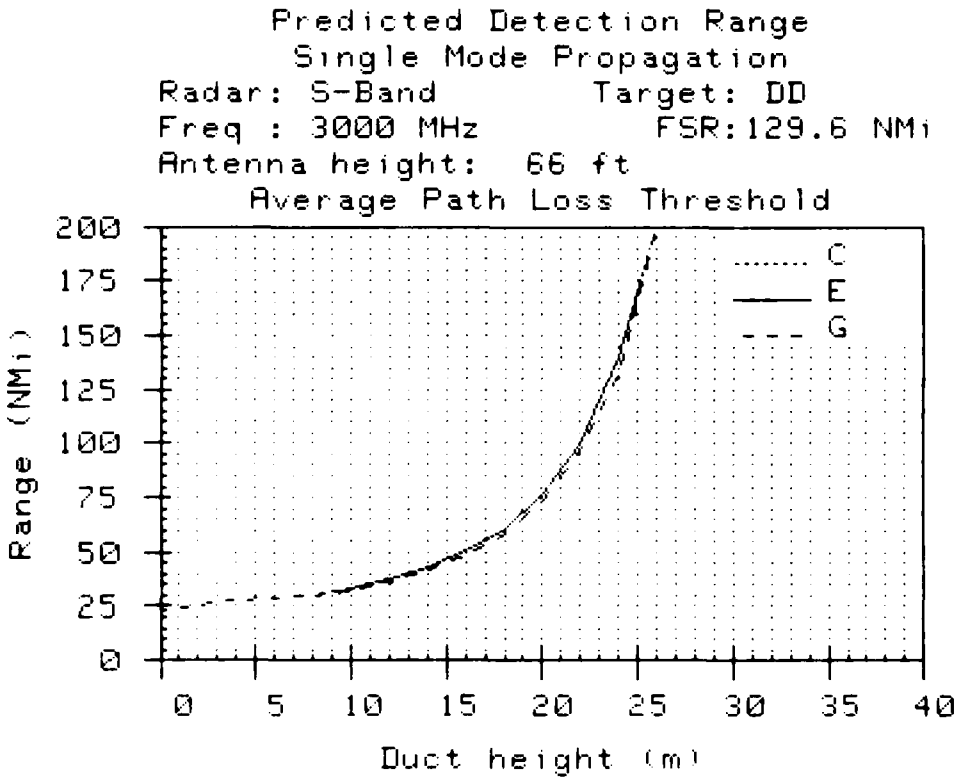

Duct Height (m)	C Model Range (NMi)	E Model Range (NMi)	G Model Range (NMi)
0.0	23.9	23.9	23.9
2.0	25.9	25.9	25.8
4.0	27.5	27.5	27.3
6.0	28.9	28.9	28.6
8.0	30.2	30.2	29.8
10.0	33.3	33.3	32.7
12.0	37.5	37.5	36.6
14.0	43.0	43.0	41.8
16.0	50.5	50.5	48.8
18.0	60.8	60.8	58.7
20.0	75.9	75.9	73.0
22.0	99.3	99.3	95.5
24.0	139.6	139.6	132.2
26.0	200.0	200.0	199.8
28.0	200.0	200.0	200.0
30.0	200.0	200.0	200.0
32.0	200.0	200.0	200.0
34.0	200.0	200.0	200.0
36.0	200.0	200.0	200.0
38.0	200.0	200.0	200.0
40.0	200.0	200.0	200.0

Figure A3

Program: MRtplt Rev:0.00

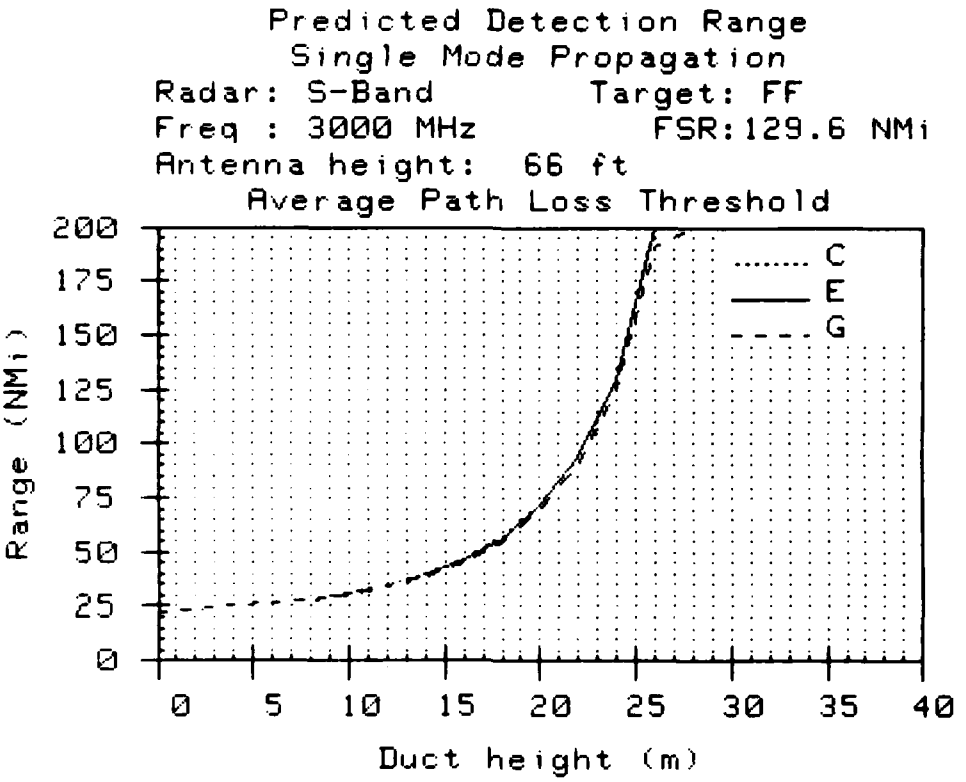

Duct Height (m)	C Model Range (NMi)	E Model Range (NMi)	G Model Range (NMi)
0.0	21.9	21.9	22.1
2.0	23.7	23.7	23.8
4.0	25.2	25.2	25.2
6.0	26.5	26.5	26.4
8.0	27.7	27.7	27.6
10.0	30.6	30.6	30.3
12.0	34.6	34.6	34.1
14.0	39.9	39.9	39.1
16.0	47.0	47.0	45.9
18.0	56.9	56.9	55.4
20.0	71.4	71.4	69.3
22.0	93.9	93.9	91.0
24.0	130.3	130.3	125.9
26.0	199.5	199.5	191.0
28.0	200.0	200.0	200.0
30.0	200.0	200.0	200.0
32.0	200.0	200.0	200.0
34.0	200.0	200.0	200.0
36.0	200.0	200.0	200.0
38.0	200.0	200.0	200.0
40.0	200.0	200.0	200.0

Figure A4

Program: MRtplt Rev:0.00

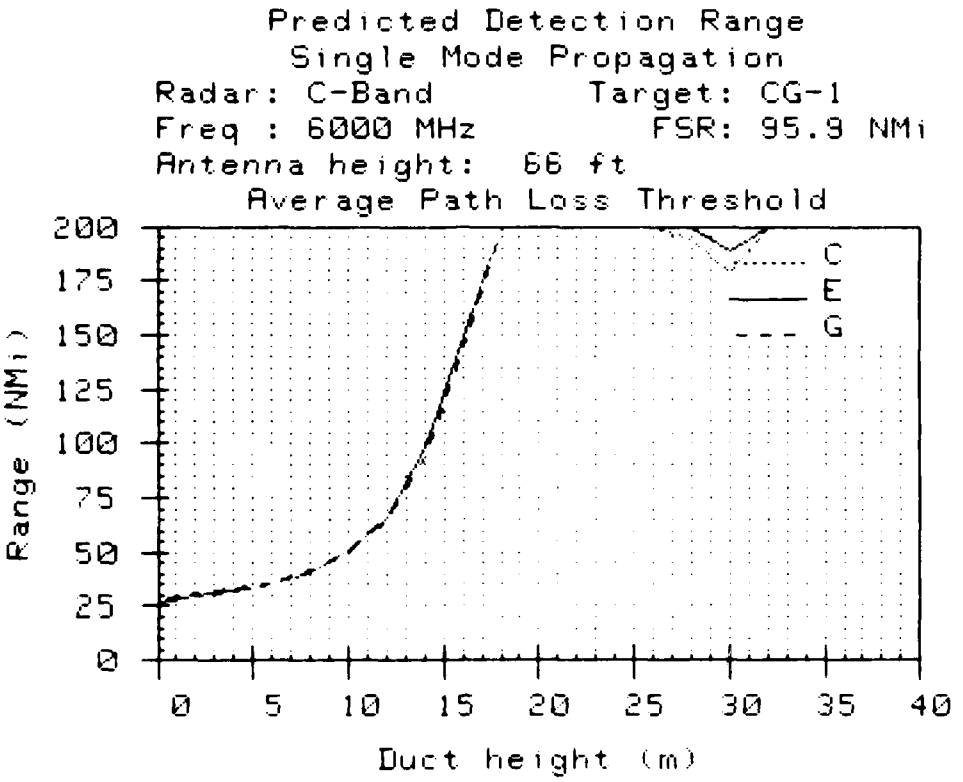

Duct Height (m)	C Model Range (NMi)	E Model Range (NMi)	G Model Range (NMi)
0.0	26.6	26.7	27.5
2.0	29.9	30.0	30.9
4.0	32.1	32.2	33.0
6.0	35.2	35.2	35.9
8.0	41.3	41.3	41.5
10.0	50.8	50.8	50.3
12.0	66.8	66.8	65.1
14.0	97.7	97.7	94.1
16.0	149.1	149.1	144.4
18.0	200.0	200.0	200.0
20.0	200.0	200.0	200.0
22.0	200.0	200.0	200.0
24.0	200.0	200.0	200.0
26.0	200.0	200.0	200.0
28.0	194.6	200.0	200.0
30.0	178.6	188.8	200.0
32.0	199.6	200.0	200.0
34.0	199.6	200.0	200.0
36.0	199.6	200.0	200.0
38.0	199.6	200.0	200.0
40.0	199.6	200.0	200.0

Figure A5

Program: MRtplt Rev:0.00

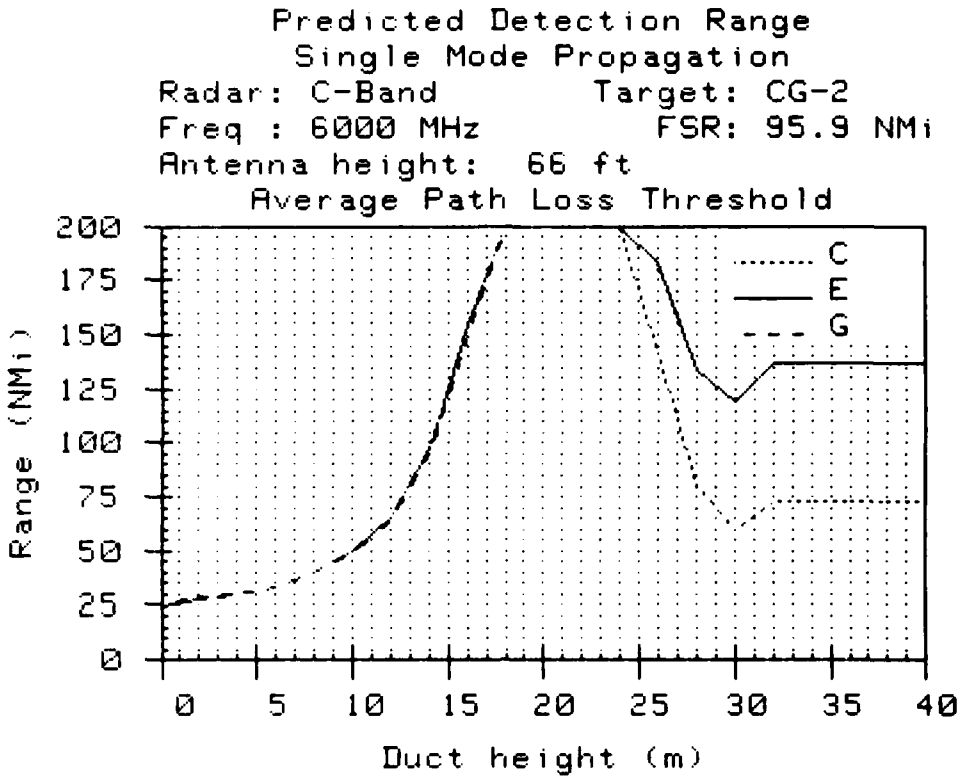

Duct Height (m)	C Model Range (NMi)	E Model Range (NMi)	G Model Range (NMi)
0.0	24.3	24.3	25.1
2.0	27.6	27.6	28.4
4.0	29.8	29.8	30.5
6.0	33.2	33.2	33.5
8.0	39.5	39.5	39.3
10.0	49.3	49.3	48.6
12.0	65.7	65.7	64.2
14.0	97.1	97.0	94.5
16.0	154.0	154.0	150.4
18.0	200.0	200.0	200.0
20.0	200.0	200.0	200.0
22.0	200.0	200.0	200.0
24.0	200.0	200.0	200.0
26.0	141.3	182.9	200.0
28.0	80.3	133.7	200.0
30.0	60.0	119.5	200.0
32.0	73.1	137.2	200.0
34.0	73.1	137.2	200.0
36.0	73.1	137.2	200.0
38.0	73.1	137.2	200.0
40.0	73.1	137.2	200.0

Figure A6

Program: MRtplt Rev:0.00

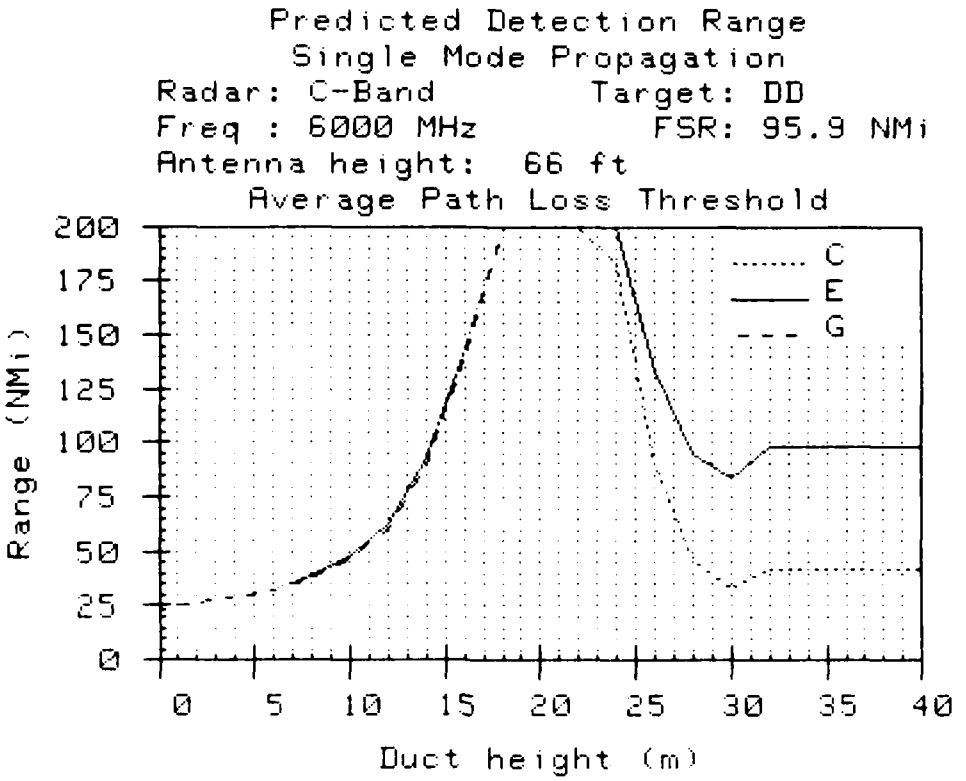

Duct Height (m)	C Model Range (NMi)	E Model Range (NMi)	G Model Range (NMi)
0.0	23.8	23.8	23.9
2.0	27.0	27.0	27.0
4.0	29.1	29.1	29.1
6.0	32.2	32.2	31.9
8.0	38.3	38.3	37.5
10.0	47.6	47.5	46.2
12.0	63.0	63.0	60.9
14.0	92.7	92.7	89.6
16.0	143.7	143.7	141.4
18.0	200.0	200.0	200.0
20.0	200.0	200.0	200.0
22.0	200.0	200.0	200.0
24.0	182.8	200.0	200.0
26.0	90.9	133.0	200.0
28.0	46.7	94.4	200.0
30.0	33.5	83.7	200.0
32.0	41.8	97.8	200.0
34.0	41.8	97.8	200.0
36.0	41.8	97.8	200.0
38.0	41.8	97.8	200.0
40.0	41.8	97.8	200.0

Figure A7

Program: MRtplt Rev:0.00

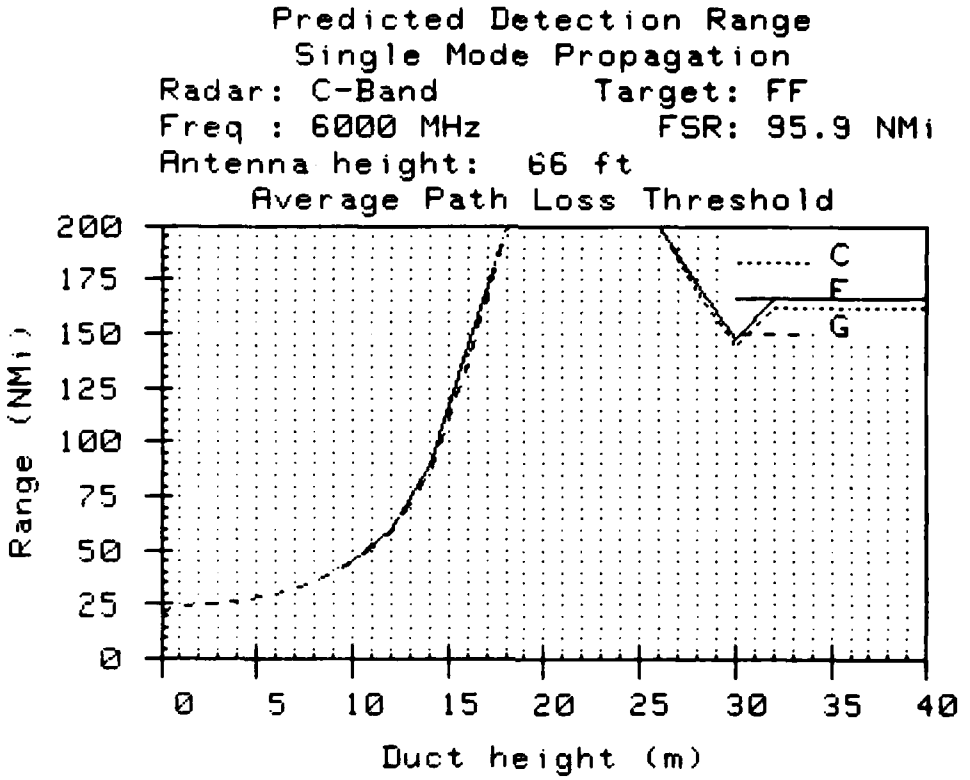

Duct Height (m)	C Model Range (NMi)	E Model Range (NMi)	G Model Range (NMi)
0.0	21.9	21.9	22.2
2.0	25.0	25.0	25.1
4.0	27.0	27.0	27.1
6.0	30.0	30.0	29.8
8.0	35.8	35.8	35.3
10.0	44.9	44.9	43.8
12.0	60.0	60.0	58.2
14.0	89.0	89.0	86.2
16.0	144.4	144.4	137.0
18.0	200.0	200.0	200.0
20.0	200.0	200.0	200.0
22.0	200.0	200.0	200.0
24.0	200.0	200.0	200.0
26.0	200.0	200.0	200.0
28.0	169.9	172.9	200.0
30.0	144.3	148.2	200.0
32.0	162.2	166.5	200.0
34.0	162.2	166.5	200.0
36.0	162.2	166.5	200.0
38.0	162.2	166.5	200.0
40.0	162.2	166.5	200.0

Figure A8

Program: MRtplt Rev:0.00

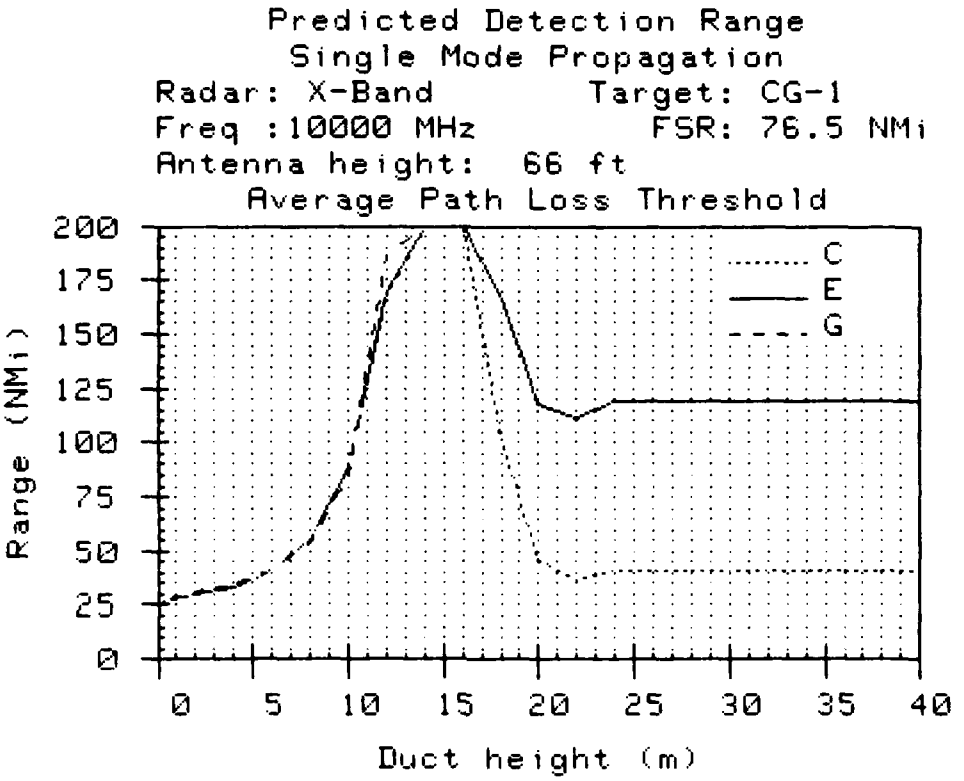

Duct Height (m)	C Model Range (NMi)	E Model Range (NMi)	G Model Range (NMi)
0.0	26.3	26.5	27.2
2.0	30.4	30.5	31.3
4.0	33.4	33.5	34.2
6.0	41.0	41.0	41.2
8.0	55.5	55.5	54.4
10.0	88.6	88.5	85.5
12.0	169.2	169.9	186.7
14.0	200.0	200.0	200.0
16.0	200.0	200.0	200.0
18.0	100.8	166.8	200.0
20.0	46.0	118.1	200.0
22.0	36.2	111.7	200.0
24.0	41.1	119.6	200.0
26.0	41.1	119.6	200.0
28.0	41.1	119.6	200.0
30.0	41.1	119.6	200.0
32.0	41.1	119.6	200.0
34.0	41.1	119.6	200.0
36.0	41.1	119.6	200.0
38.0	41.1	119.6	200.0
40.0	41.1	119.6	200.0

Figure A9

Program: MRtplt Rev:0.00

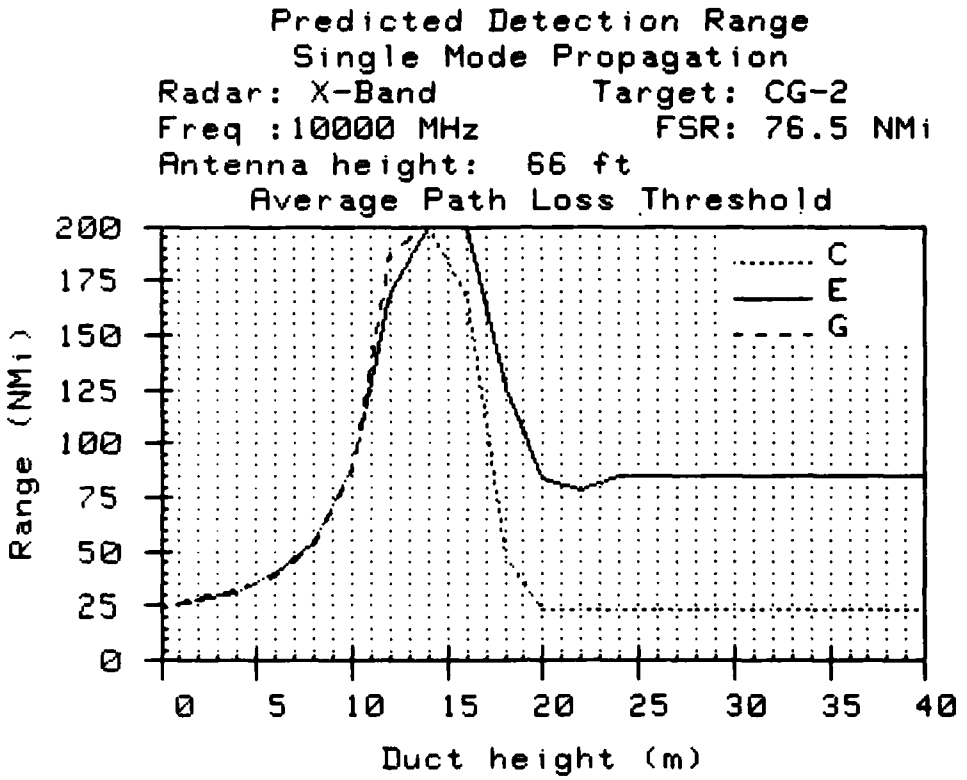

Duct Height (m)	C Model Range (NMi)	E Model Range (NMi)	G Model Range (NMi)
0.0	24.0	24.1	24.9
2.0	28.0	28.0	28.9
4.0	31.4	31.5	31.9
6.0	39.5	39.5	39.3
8.0	54.5	54.5	53.4
10.0	88.6	88.6	86.9
12.0	169.6	170.3	188.0
14.0	200.0	200.0	200.0
16.0	168.0	200.0	200.0
18.0	47.8	125.5	200.0
20.0	23.5	83.9	200.0
22.0	23.0	78.5	200.0
24.0	23.2	84.9	200.0
26.0	23.2	84.9	200.0
28.0	23.2	84.9	200.0
30.0	23.2	84.9	200.0
32.0	23.2	84.9	200.0
34.0	23.2	84.9	200.0
36.0	23.2	84.9	200.0
38.0	23.2	84.9	200.0
40.0	23.2	84.9	200.0

Figure A10

Program: MRtplt Rev:0.00

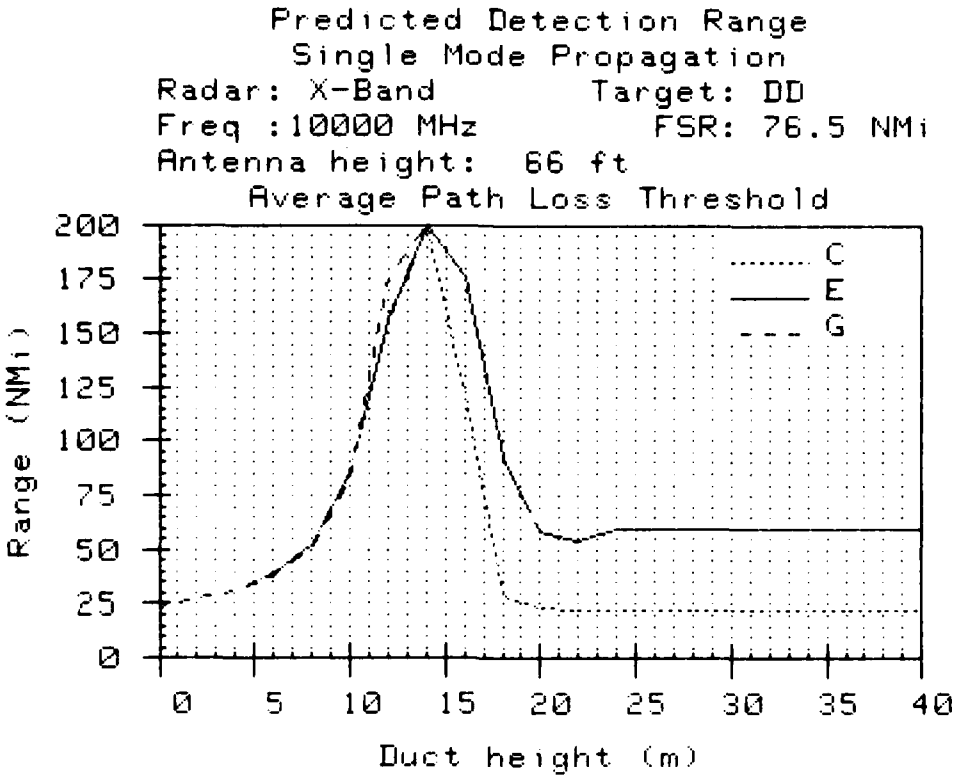

Duct Height (m)	C Model Range (NMi)	E Model Range (NMi)	G Model Range (NMi)
0.0	23.6	23.6	23.8
2.0	27.5	27.5	27.7
4.0	30.7	30.7	30.6
6.0	38.3	38.3	37.6
8.0	52.5	52.5	51.0
10.0	84.7	84.7	82.8
12.0	156.0	156.7	176.8
14.0	200.0	200.0	200.0
16.0	121.4	176.7	200.0
18.0	28.5	92.2	200.0
20.0	22.9	58.6	200.0
22.0	22.4	54.4	200.0
24.0	22.5	59.4	200.0
26.0	22.5	59.4	200.0
28.0	22.5	59.4	200.0
30.0	22.5	59.4	200.0
32.0	22.5	59.4	200.0
34.0	22.5	59.4	200.0
36.0	22.5	59.4	200.0
38.0	22.5	59.4	200.0
40.0	22.5	59.4	200.0

Figure A11

Program: MRtplt Rev:0.00

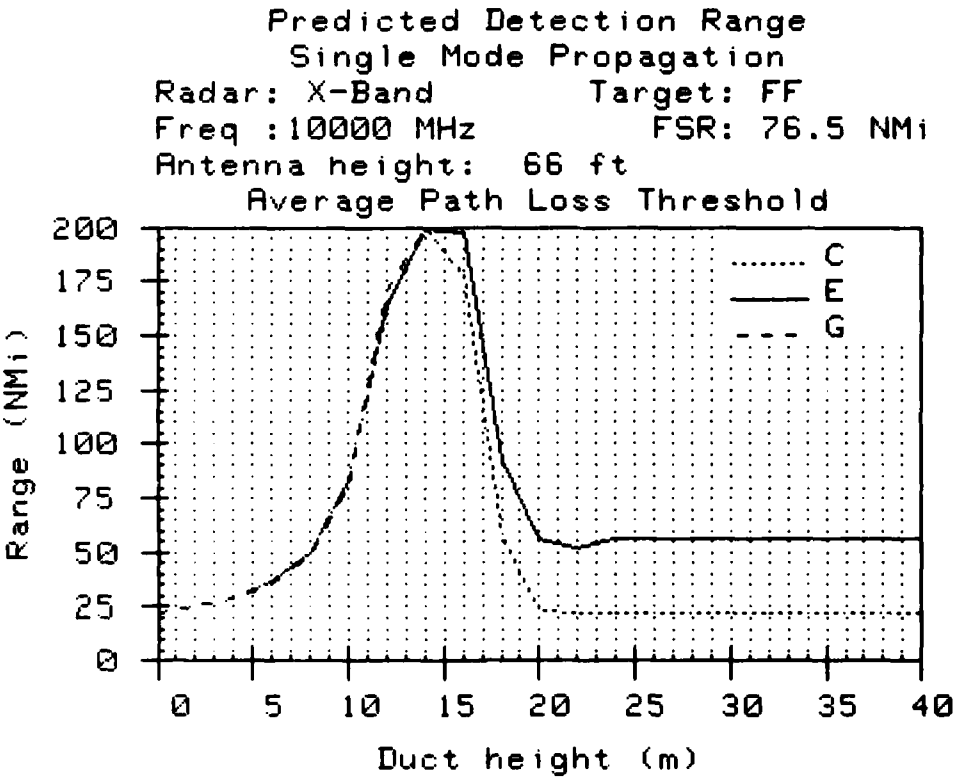

Duct Height (m)	C Model Range (NMi)	E Model Range (NMi)	G Model Range (NMi)
0.0	21.8	21.8	22.2
2.0	25.6	25.6	26.0
4.0	28.7	28.7	28.7
6.0	36.2	36.2	35.6
8.0	50.2	50.2	48.9
10.0	83.2	83.1	80.4
12.0	164.6	164.8	171.4
14.0	200.0	200.0	200.0
16.0	178.0	197.1	200.0
18.0	57.0	93.0	200.0
20.0	23.0	56.2	200.0
22.0	22.4	51.7	200.0
24.0	22.7	56.6	200.0
26.0	22.7	56.6	200.0
28.0	22.7	56.6	200.0
30.0	22.7	56.6	200.0
32.0	22.7	56.6	200.0
34.0	22.7	56.6	200.0
36.0	22.7	56.6	200.0
38.0	22.7	56.6	200.0
40.0	22.7	56.6	200.0

Figure A12

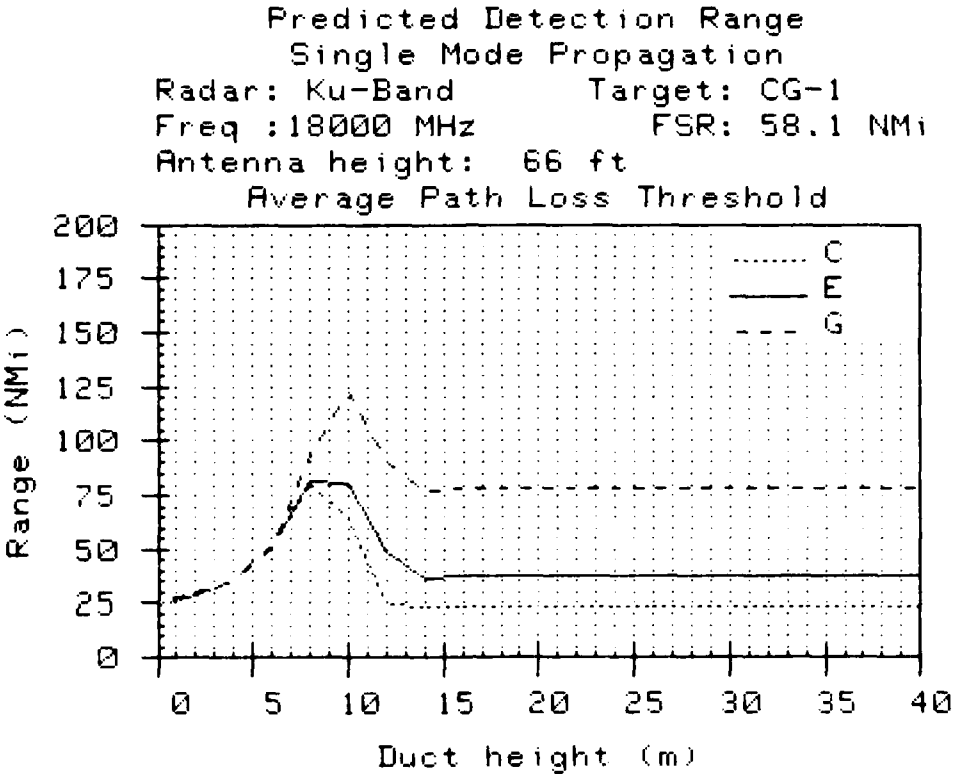

Duct Height (m)	C Model Range (NMi)	E Model Range (NMi)	G Model Range (NMi)
0.0	24.9	25.1	25.7
2.0	29.2	29.3	30.1
4.0	35.3	35.4	35.6
6.0	52.0	52.0	50.7
8.0	80.6	81.6	94.1
10.0	63.8	81.1	122.3
12.0	24.7	48.8	90.3
14.0	23.7	36.8	77.2
16.0	23.6	37.7	78.6
18.0	23.6	37.7	78.6
20.0	23.6	37.7	78.6
22.0	23.6	37.7	78.6
24.0	23.6	37.7	78.6
26.0	23.6	37.7	78.6
28.0	23.6	37.7	78.6
30.0	23.6	37.7	78.6
32.0	23.6	37.7	78.6
34.0	23.6	37.7	78.6
36.0	23.6	37.7	78.6
38.0	23.6	37.7	78.6
40.0	23.6	37.7	78.6

Figure A13

Program: MRtplt Rev. 0.00

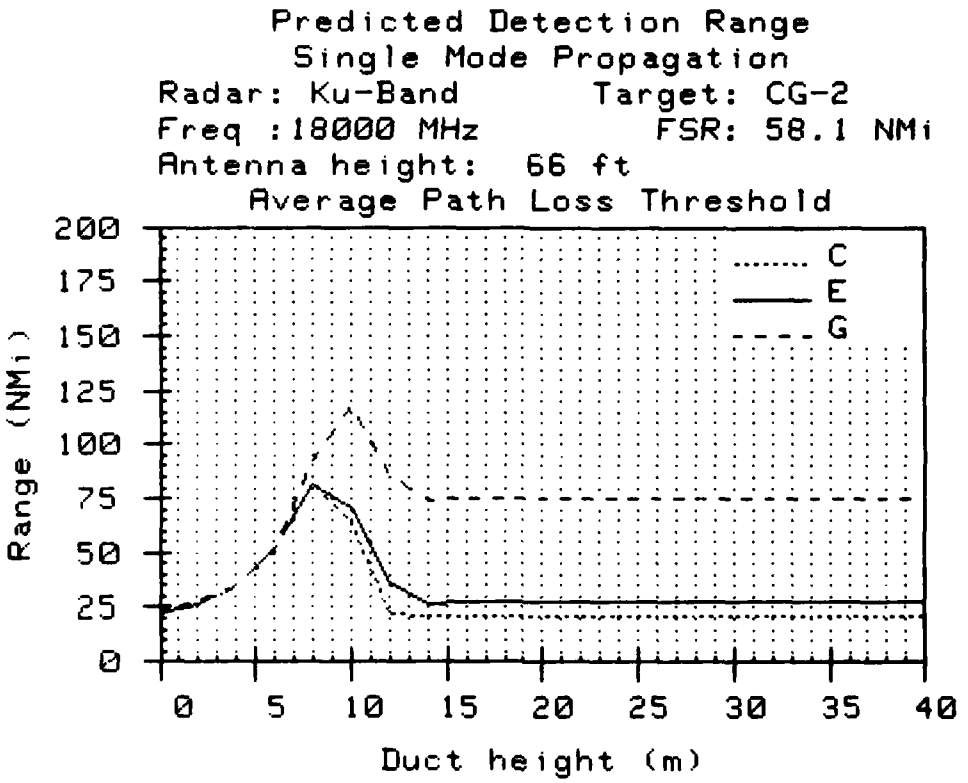

Duct Height (m)	C Model Range (NMi)	E Model Range (NMi)	G Model Range (NMi)
0.0	22.6	22.6	23.6
2.0	27.1	27.1	28.0
4.0	34.1	34.1	34.0
6.0	51.5	51.5	50.6
8.0	81.3	81.7	92.6
10.0	63.9	71.2	118.5
12.0	22.6	37.1	86.6
14.0	21.0	26.8	73.6
16.0	20.9	27.8	75.0
18.0	20.9	27.8	75.0
20.0	20.9	27.8	75.0
22.0	20.9	27.8	75.0
24.0	20.9	27.8	75.0
26.0	20.9	27.8	75.0
28.0	20.9	27.8	75.0
30.0	20.9	27.8	75.0
32.0	20.9	27.8	75.0
34.0	20.9	27.8	75.0
36.0	20.9	27.8	75.0
38.0	20.9	27.8	75.0
40.0	20.9	27.8	75.0

Figure A14

Program: MRtplt Rev:0.00

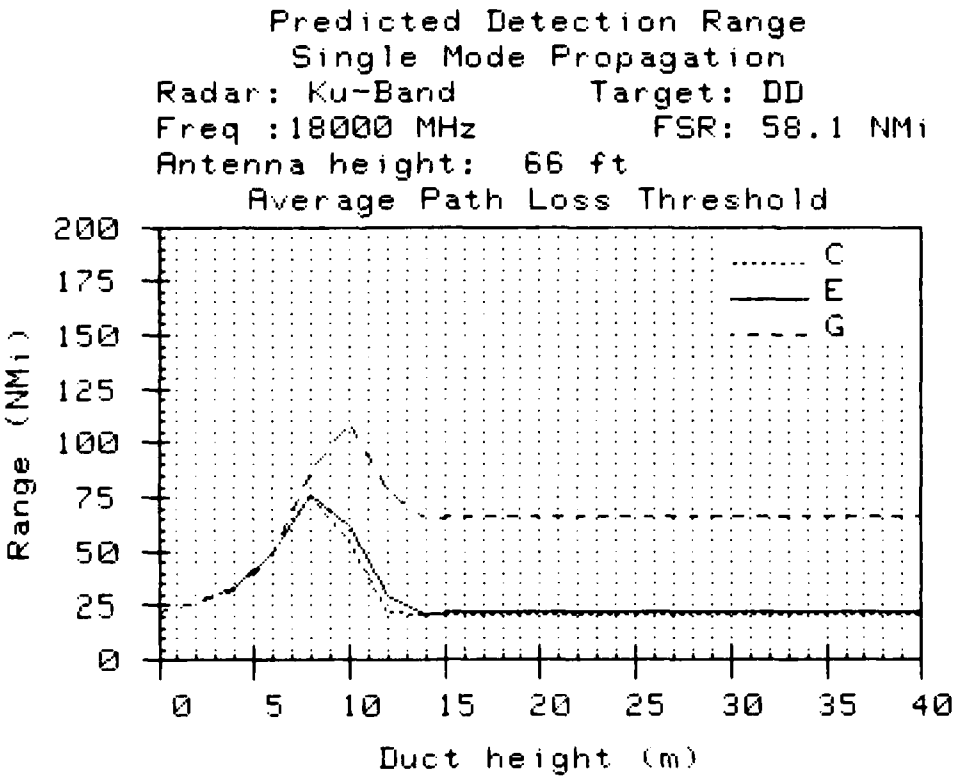

Duct Height (m)	C Model Range (NMi)	E Model Range (NMi)	G Model Range (NMi)
0.0	22.3	22.3	22.6
2.0	26.7	26.7	26.9
4.0	33.2	33.2	32.7
6.0	49.7	49.7	48.4
8.0	75.7	76.1	87.7
10.0	54.0	61.6	109.2
12.0	22.2	29.8	77.9
14.0	20.8	21.6	65.3
16.0	20.7	21.9	66.6
18.0	20.7	21.9	66.6
20.0	20.7	21.9	66.6
22.0	20.7	21.9	66.6
24.0	20.7	21.9	66.6
26.0	20.7	21.9	66.6
28.0	20.7	21.9	66.6
30.0	20.7	21.9	66.6
32.0	20.7	21.9	66.6
34.0	20.7	21.9	66.6
36.0	20.7	21.9	66.6
38.0	20.7	21.9	66.6
40.0	20.7	21.9	66.6

Figure A15

Program: MRtplt Rev:0.00

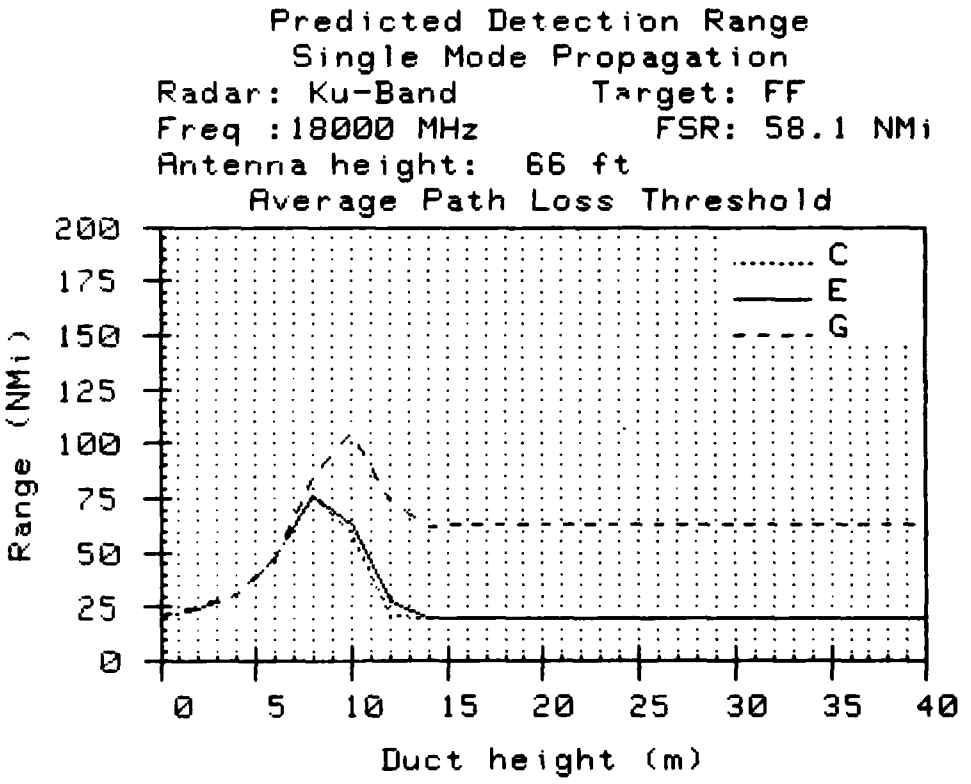

Duct Height (m)	C Model Range (NMi)	E Model Range (NMi)	G Model Range (NMi)
0.0	20.7	20.7	21.1
2.0	25.0	25.0	25.4
4.0	31.5	31.5	31.2
6.0	48.0	48.0	46.9
8.0	76.5	76.7	85.4
10.0	58.8	63.1	104.9
12.0	21.4	27.6	73.9
14.0	19.6	20.2	61.5
16.0	19.5	20.3	62.8
18.0	19.5	20.3	62.8
20.0	19.5	20.3	62.8
22.0	19.5	20.3	62.8
24.0	19.5	20.3	62.8
26.0	19.5	20.3	62.8
28.0	19.5	20.3	62.8
30.0	19.5	20.3	62.8
32.0	19.5	20.3	62.8
34.0	19.5	20.3	62.8
36.0	19.5	20.3	62.8
38.0	19.5	20.3	62.8
40.0	19.5	20.3	62.8

Figure A16

APPENDIX B

Figures B1 through B16 list the percent occurrence of detection range exceeding 60 nmi for each of the 212 Marsden Squares contained in the cutoff duct height climatology. These figures show the results for computations made using the modified single mode propagation model with the conservative RCS model. Columns on the figure are degrees latitude and rows are degrees longitude. Probability within a 10° grid is found at the intersection of the desired latitude column and longitude row. The average, rms and standard deviation of the total distribution are also included with each figure.

Program: SMRPC Rev:2.10

Modified Single Mode - Conservative RCS Model
Percent Exceeding 60 NMi Detection Range
Radar: S-Band Target: CG-1 [Avg]
Freq: 3000 MHz FSR:129.6 NMi
Antenna Height: 66 ft Cut: ON

Long.	Latitude (deg)															
(deg)	-75	-65	-55	-45	-35	-25	-15	-05	05	15	25	35	45	55	65	75
175								24	25	33	25	12	2	1		
165									27	32	26	11	2	1		
155									28	29	27	11	3	1		
145									24	27	23	12	3	1		
135									23	26	19	11	3	2		
125									21	28	14	6	3	2		
115									19	27	12	7				
105									19	22	20					
95								15	16	20	25					
85								8	13		29					
75			2	3	5	10	9			32	29	20				
65			2	5						33	28	22	4			
55				4	8					34	25	19	6	1		
45					15	14			28	32	24	17	7	2		
35						20	25	28	25	31	23	15	9	2	1	
25									22	24	24	13	8	3	2	
15								26	17	16	15	14	7	3	2	
5							26	22	17			10	6	3	1	
-5						17	21	17	16			12	9	3	1	
-15					11	11	6					13	10	3		
-25					16							15	9			
-35					21	25	26				27	16	6			
-45						24	23	24		22						
-55						26			24	19	17					
-65									30	28	21					
-75								25	24	24						
-85									27	25						
-95							30	20	22	23						
-105						26	32	23	23							
-115					18	27	26	21	24	27	20					
-125					10			22	27	28	25	14				
-135					9			25	26	31	24	20	5			
-145								22	28	33	24	18	4			
-155					17	28	29	24	26	32	24	15	3	2		
-165					13	23	29		27	32	24	13	2	1		
-175					10		28		21	33	24	13	3	1		

Counts : 212.0 Sum %: 3.562E+03 (Sum %)^2: 7.982E+04
Average %: 16.8 RMS %: 1.940E+01 Std Dev : 9.731E+00

Figure B1

Program: SMRPC Rev:2.10

Modified Single Mode - Conservative RCS Model
Percent Exceeding 60 NMi Detection Range
Radar: S-Band Target: CG-2 [Avg]
Freq: 3000 MHz FSR:129.6 NMi
Antenna Height: 66 ft Cut: ON

Long.	Latitude (deg)															
(deg)	-75	-65	-55	-45	-35	-25	-15	-05	05	15	25	35	45	55	65	75
175								21	23	29	22	10	2	1		
165									24	28	23	10	2	1		
155									24	26	23	10	2	1		
145									22	24	20	10	2	1		
135									20	23	17	9	3	2		
125									18	25	13	5	3	2		
115									17	24	11	6				
105									16	20	17					
95								13	14	18	22					
85								7	11		26					
75			1	3	4	9	8			29	25	18				
65			2	4						30	25	20	4			
55				3	7					30	22	17	5	1		
45					13	12			25	28	21	15	6	1		
35						18	22	25	22	27	21	13	7	2	1	
25									19	21	22	12	7	3	2	
15								23	15	14	13	13	6	3	1	
5							23	19	15			9	5	3	1	
-5						15	19	14	14			10	8	3	1	
-15					10	9	5					12	9	2		
-25					14							13	8			
-35					18	22	23				24	16	5			
-45						22	20	21		19						
-55						23			21	17	15					
-65									27	25	19					
-75								22	22	21						
-85									24	23						
-95							26	18	19	20						
-105						23	29	20	21							
-115					16	24	23	18	21	24	18					
-125					9			19	20	25	22	13				
-135					8			22	23	28	21	18	5			
-145								20	25	30	22	15	4			
-155					15	25	26	21	23	29	21	13	2	1		
-165					11	21	26		24	29	21	12	2	1		
-175					9		25		18	29	21	11	2	1		

Counts : 212.0 Sum %: 3.132E+03 (Sum %)^2: 6.206E+04
Average %: 14.8 RMS %: 1.711E+01 Std Dev : 8.650E+00

Figure B2

Program: SMRPC Rev:2.10

Modified Single Mode - Conservative RCS Model
Percent Exceeding 60 NMi Detection Range
Radar: S-Band Target: FF [Avg]
Freq: 3000 MHz FSR:129.6 NMi
Antenna Height: 66 ft Cut: ON

Long.	Latitude (deg)															
(deg)	-75	-65	-55	-45	-35	-25	-15	-05	05	15	25	35	45	55	65	75
175								12	14	17	13	6	1	1		
165									14	16	13	5	1	1		
155									14	15	13	5	1	1		
145									13	14	11	6	1	1		
135									11	13	10	5	2	1		
125									10	14	7	3	2	1		
115									9	14	6	3				
105									10	11	10					
95								7	8	10	13					
85								4	6		15					
75			1	2	2	5	5			17	15	11				
65			1	2						18	15	11	2			
55				2	4					18	13	10	3	1		
45					7	7			14	17	12	9	4	1		
35						10	13	14	12	16	12	7	4	1	1	
25									11	12	13	7	4	1	1	
15								13	8	8	7	7	3	2	1	
5							13	11	8			5	3	1	1	
-5						9	11	8	8			6	5	1	1	
-15					6	5	3					7	5	1		
-25					8							8	4			
-35					11	13	13				15	9	3			
-45						13	12	12		11						
-55						13			12	10	9					
-65									16	15	11					
-75								13	13	13						
-85									14	14						
-95							16	10	11	11						
-105						14	18	11	12							
-115					9	14	13	11	12	15	10					
-125					5			11	12	15	13	7				
-135					4			13	13	17	13	11	3			
-145								12	15	18	13	9	2			
-155					9	15	16	12	13	17	12	8	1	1		
-165					6	12	15		14	17	12	7	1	1		
-175					5		15		11	18	12	6	1	1		

Counts : 212.0 Sum %: 1.781E+03 (Sum %)^2: 2.044E+04
Average %: 8.4 RMS %: 9.818E+00 Std Dev : 5.097E+00

Figure B3

Program: SMRPC Rev:2.10

Modified Single Mode - Conservative RCS Model
Percent Exceeding 60 NMi Detection Range
Radar: S-Band Target: DD [Avg]
Freq: 3000 MHz FSR:129.6 NMi
Antenna Height: 66 ft Cut: ON

Long.	Latitude (deg)															
(deg)	-75	-65	-55	-45	-35	-25	-15	-05	05	15	25	35	45	55	65	75
175								17	19	23	17	8	2	1		
165									19	22	18	7	2	1		
155									19	20	19	7	2	1		
145									17	19	16	8	2	1		
135									16	18	13	7	2	1		
125									14	20	9	4	2	2		
115									13	19	8	4				
105									13	15	14					
95								10	11	14	18					
85								5	8		21					
75			1	2	3	6	6			23	20	15				
65			1	3						24	20	16	3			
55				3	5					24	17	13	4	1		
45					10	10			20	23	17	12	5	1		
35						14	17	20	17	22	16	10	6	1	1	
25									15	16	17	9	6	2	1	
15								18	11	11	10	10	4	2	1	
5							18	15	11			7	4	2	1	
-5						12	15	11	11			8	6	2	1	
-15					8	7	4					9	7	2		
-25					11							10	6			
-35					15	17	18				20	13	4			
-45						17	16	17		15						
-55						18			17	14	13					
-65									22	20	15					
-75								17	17	17						
-85									19	19						
-95							21	14	15	16						
-105						19	24	16	17							
-115					12	19	18	15	17	20	14					
-125					7			15	16	20	18	10				
-135					6			17	18	23	17	14	4			
-145								16	20	24	18	12	3			
-155					12	20	21	17	18	23	17	10	2	1		
-165					9	16	21		19	23	17	9	2	1		
-175					7		20		15	24	17	8	2	1		

Counts : 212.0 Sum %: 2.469E+03 (Sum %)^2: 3.907E+04
Average %: 11.6 RMS %: 1.358E+01 Std Dev : 6.990E+00

Figure B4

Program: SMRPC Rev:2.10

Modified Single Mode - Conservative RCS Model
Percent Exceeding 60 NMi Detection Range
Radar: C-Band Target: CG-1 [Avg]
Freq: 6000 MHz FSR: 95.9 NMi
Antenna Height: 66 ft Cut: ON

Long.	Latitude (deg)															
(deg)	-75	-65	-55	-45	-35	-25	-15	-05	05	15	25	35	45	55	65	75
175								69	70	80	69	44	16	5		
165									76	82	73	43	15	5		
155									75	78	74	44	16	7		
145									72	74	71	49	18	9		
135									70	75	67	49	21	13		
125									69	77	61	32	16	12		
115									66	77	51	35				
105									63	66	63					
95								54	64	62	65					
85								42	56		73					
75			9	24	25	50	39			77	73	57				
65			13	24						80	74	64	19			
55				17	33					81	71	60	25	4		
45					51	48			77	78	70	57	31	11		
35						63	72	76	74	79	71	53	39	15	10	
25									70	72	71	50	37	26	11	
15								72	62	59	54	55	36	23	11	
5							76	71	64			42	31	20	8	
-5						63	72	69	66			46	38	20	12	
-15					44	43	36					49	39	14		
-25					54							53	36			
-35					63	70	71				66	60	30			
-45						68	67	71		62						
-55						72			66	57	51					
-65									75	71	60					
-75								71	67	67						
-85									72	68						
-95							75	66	67	67						
-105						74	77	70	67							
-115					65	72	70	65	68	71	60					
-125					48			64	68	72	67	48				
-135					46			70	72	77	65	59	22			
-145								66	74	78	66	56	18			
-155					57	72	75	69	73	78	67	53	15	6		
-165					48	67	73		71	78	67	48	13	5		
-175					40		74		58	78	68	46	15	5		

Counts : 212.0 Sum %: 1.122E+04 (Sum %)^2: 6.999E+05
Average %: 52.9 RMS %: 5.746E+01 Std Dev : 2.244E+01

Figure B5

Program: SMRPC Rev:2.10

Modified Single Mode - Conservative RCS Model
Percent Exceeding 60 NMi Detection Range
Radar: C-Band Target: CG-2 [Avg]
Freq: 6000 MHz FSR: 95.9 NMi
Antenna Height: 66 ft Cut: ON

Long. (deg)	Latitude (deg)														
	-75	-65	-55	-45	-35	-25	-15	-05	05	15	25	35	45	55	65	75
175								68	69	80	69	43	15	5		
165									75	81	72	42	14	5		
155									74	77	74	43	15	7		
145									71	73	70	48	17	8		
135									69	74	66	48	20	13		
125									68	76	60	31	16	12		
115									65	76	50	34				
105									62	65	63					
95								53	63	61	64					
85								40	55		72					
75			9	23	24	49	39			76	73	56				
65			12	24						79	74	63	19			
55				17	32					81	71	59	24	4		
45					50	47			76	77	69	56	30	10		
35						62	71	75	73	78	70	52	38	14	9	
25									69	71	70	49	36	24	10	
15								71	61	58	53	54	35	22	10	
5							75	70	63			41	30	19	8	
-5						62	70	68	65			45	37	19	12	
-15					43	42	35					48	38	13		
-25					53							52	35			
-35					62	69	70				65	59	29			
-45						67	67	70		61						
-55						72			66	56	50					
-65									74	71	60					
-75								70	66	66						
-85									71	67						
-95							74	65	66	67						
-105						73	77	69	66							
-115					64	71	69	64	67	70	59					
-125					47			63	67	71	66	47				
-135					45			70	71	76	64	58	22			
-145								65	74	77	66	55	17			
-155					56	71	74	68	72	78	66	52	14	6		
-165					47	66	72		70	77	66	47	13	5		
-175					39		73		57	78	67	45	15	5		

Counts : 212.0 Sum %: 1.104E+04 (Sum %)^2: 6.803E+05
Average %: 52.1 RMS %: 5.665E+01 Std Dev : 2.237E+01

Figure B6

Program: SMRPC Rev:2.10

Modified Single Mode - Concervative RCS Model
Percent Exceeding 60 NMi Detection Range
Radar: C-Band Target: DD [Avg]
Freq: 6000 MHz FSR: 95.9 NMi
Antenna Height: 66 ft Cut: ON

Long. (deg)	Latitude (deg)															
	-75	-65	-55	-45	-35	-25	-15	-05	05	15	25	35	45	55	65	75
175								66	68	78	67	41	14	5		
165									73	80	70	40	13	4		
155									72	75	72	41	14	6		
145									70	72	68	46	15	7		
135									67	72	64	46	19	11		
125									66	75	57	29	14	11		
115									63	75	47	32				
105									60	63	61					
95								51	60	59	62					
85								38	53		70					
75			8	21	22	46	37			75	71	55				
65			11	22						78	72	61	18			
55				16	30					79	69	57	23	3		
45					48	45			75	76	68	54	29	9		
35						60	69	74	71	77	68	50	36	13	8	
25									67	69	68	47	34	22	9	
15								69	59	56	51	51	33	20	9	
5							74	68	61			39	28	17	7	
-5						59	68	66	63			43	35	17	10	
-15					41	40	33					46	36	12		
-25					51							50	33			
-35					60	67	69				64	57	27			
-45						65	65	68		59						
-55						70			64	54	49					
-65									73	69	58					
-75								68	65	65						
-85									70	66						
-95							73	63	65	65						
-105						71	75	68	65							
-115					62	69	67	63	66	69	57					
-125					45			62	65	70	64	45				
-135					42			68	70	74	62	57	20			
-145								63	72	76	64	53	16			
-155					55	70	72	66	71	76	64	50	13	5		
-165					45	65	71		68	76	64	45	12	5		
-175					37		72		56	76	66	43	13	4		

Counts : 212.0 Sum %: 1.068E+04 (Sum %)^2: 6.426E+05
Average %: 50.4 RMS %: 5.506E+01 Std Dev : 2.223E+01

Figure B7

Program: SMRPC Rev:2.10

Modified Single Mode - Conservative RCS Model
Percent Exceeding 60 NMi Detection Range
Radar: C-Band Target: FF [Avg]
Freq: 6000 MHz FSR: 95.9 NMi
Antenna Height: 66 ft Cut: ON

Long.	Latitude (deg)														
(deg)	-75	-65	-55	-45	-35	-25	-15	-05	05	15	25	35	45	55	65	75
175								64	66	77	65	39	12	4		
165									71	78	68	38	11	3		
155									70	73	70	39	12	5		
145									67	70	66	44	13	6		
135									65	70	61	43	16	10		
125									63	73	54	27	13	9		
115									60	73	44	29				
105									58	61	58					
95								48	58	57	60					
85								35	50		69					
75			6	18	20	43	34			73	69	53				
65			9	20						76	70	59	16			
55				14	28					78	67	55	21	3		
45					46	43			73	74	65	52	27	8		
35						57	67	72	68	75	66	47	33	11	7	
25									64	67	66	45	32	19	8	
15								67	57	53	48	49	30	18	8	
5							71	65	59			36	25	15	6	
-5						56	66	62	60			40	33	15	8	
-15					38	38	30					44	34	11		
-25					49							48	31			
-35					58	65	67				62	54	25			
-45						63	63	66		58						
-55						68			62	52	47					
-65									71	67	56					
-75								66	62	63						
-85									68	64						
-95							71	60	62	63						
-105						69	73	66	63							
-115					59	67	65	60	63	67	55					
-125					42			59	63	68	62	43				
-135					39			66	68	72	60	54	18			
-145								61	70	74	62	51	15			
-155					52	68	70	64	69	75	62	48	12	5		
-165					43	63	69		67	74	62	43	10	4		
-175					35		70		54	74	64	41	12	4		

Counts : 212.0 Sum %: 1.023E+04 (Sum %)^2: 5.958E+05
Average %: 48.2 RMS %: 5.301E+01 Std Dev : 2.205E+01

Figure B8

Program: SMRPC Rev:2.10

Modified Single Mode - Conservative RCS Model
Percent Exceeding 60 NMi Detection Range
Radar: X-Band Target: CG-1 [Avg]
Freq: 10000 MHz FSR: 76.5 NMi
Antenna Height: 66 ft Cut: ON

Long. (deg)	Latitude (deg)															
	-75	-65	-55	-45	-35	-25	-15	-05	05	15	25	35	45	55	65	75
175								83	83	90	83	60	31	14		
165									89	92	86	60	30	13		
155									89	90	87	61	31	18		
145									87	87	85	68	35	22		
135									86	87	83	69	40	29		
125									85	89	80	52	32	26		
115									83	89	71	58				
105									80	80	78					
95								72	81	75	77					
85								63	76		84					
75			25	45	45	72	56			87	85	70				
65			28	42						90	86	78	31			
55				30	49					91	85	76	37	10		
45					68	65			88	89	85	74	46	25		
35						80	85	88	88	90	84	71	56	32	27	
25									85	87	85	68	55	48	26	
15								85	79	76	72	74	56	45	26	
5							89	86	80			61	51	39	23	
-5						81	87	87	83			65	55	38	34	
-15					62	62	58					68	59	25		
-25					70							71	54			
-35					78	84	84				79	77	47			
-45						82	81	84		74						
-55						86			80	70	66					
-65									86	83	75					
-75								86	80	81						
-85									84	81						
-95							87	81	82	81						
-105						87	88	84	82							
-115					83	85	83	80	82	83	75					
-125					69			79	82	84	80	63				
-135					68			84	84	87	78	74	39			
-145								81	87	88	80	71	31			
-155					73	85	87	83	86	88	80	69	28	9		
-165					66	81	85		83	88	80	64	27	15		
-175					57		86		72	88	82	62	30	14		

Counts : 212.0 Sum %: 1.436E+04 (Sum %)^2: 1.073E+06
Average %: 67.7 RMS %: 7.114E+01 Std Dev : 2.183E+01

Figure B9

Program: SMRPC Rev:2.10

Modified Single Mode - Conservative RCS Model
Percent Exceeding 60 NMi Detection Range
Radar: X-Band Target: CG-2 [Avg]
Freq: 10000 MHz FSR: 76.5 NMi
Antenna Height: 66 ft Cut: ON

Long.	Latitude (deg)															
(deg)	-75	-65	-55	-45	-35	-25	-15	-05	05	15	25	35	45	55	65	75
175								83	83	90	83	60	30	14		
165									89	91	85	59	30	13		
155									89	90	87	61	31	18		
145									87	87	85	67	34	22		
135									85	87	82	69	39	29		
125									85	89	80	52	31	26		
115									83	88	71	58				
105									80	79	78					
95								72	80	75	77					
85								62	76		83					
75			25	45	44	71	56			87	85	70				
65			27	42						89	86	78	31			
55				30	49					91	85	76	37	10		
45					67	65			88	89	84	74	45	25		
35						80	85	87	88	90	84	70	56	32	27	
25									85	86	85	68	55	47	25	
15								85	79	76	71	73	56	44	25	
5							89	86	80			61	51	39	23	
-5						81	87	87	83			65	55	38	34	
-15					62	61	58					67	59	25		
-25					70							71	54			
-35					78	83	84				79	76	47			
-45						82	81	84		74						
-55						86			79	70	66					
-65									86	83	74					
-75								86	80	81						
-85									84	81						
-95							87	81	82	81						
-105						87	88	84	81							
-115					82	85	83	80	82	83	75					
-125					69			79	81	84	80	63				
-135					68			84	84	87	78	74	39			
-145								81	87	88	79	71	30			
-155					72	85	87	83	86	88	79	68	28	9		
-165					65	81	85		83	88	80	64	26	14		
-175					57		85		72	88	81	62	29	14		

Counts : 212.0 Sum %: 1.431E+04 (Sum %)^2: 1.066E+06
Average %: 67.5 RMS %: 7.092E+01 Std Dev : 2.187E+01

Figure B10

Program: SMRPC Rev:2.10

Modified Single Mode - Conservative RCS Model
Percent Exceeding 60 NMi Detection Range
Radar: X-Band Target: DD [Avg]
Freq: 10000 MHz FSR: 76.5 NMi
Antenna Height: 66 ft Cut: ON

Long.	Latitude (deg)															
(deg)	-75	-65	-55	-45	-35	-25	-15	-05	05	15	25	35	45	55	65	75
175								82	82	89	82	59	30	13		
165									88	91	85	58	29	13		
155									88	89	86	60	30	17		
145									86	87	85	66	33	21		
135									85	87	82	68	38	28		
125									84	88	79	51	31	25		
115									82	88	70	57				
105									79	79	78					
95								71	80	75	77					
85								61	75		83					
75			24	43	43	70	55				87	84	69			
65			27	41							89	86	77	30		
55				29	48						90	84	75	36	10	
45					67	64			88	88	84	73	45	24		
35						79	85	87	87	89	83	69	55	31	26	
25									84	86	84	67	54	46	25	
15								84	78	75	71	72	55	43	24	
5							88	85	80			60	50	38	22	
-5						80	87	86	82			64	54	37	32	
-15					61	60	57					66	58	25		
-25					69							70	53			
-35					77	83	83				78	76	46			
-45						82	80	84		73						
-55						85			79	69	65					
-65									85	83	74					
-75								85	80	80						
-85									84	81						
-95							86	80	81	81						
-105						86	88	83	81							
-115					82	84	82	80	81	83	74					
-125					68			78	81	83	79	62				
-135					67			83	83	87	77	73	38			
-145								80	86	88	79	70	30			
-155					72	85	86	82	85	88	79	68	27	9		
-165					64	80	85		82	87	79	63	26	14		
-175					56		85		71	88	81	61	28	13		

Counts : 212.0 Sum %: 1.416E+04 (Sum %)^2: 1.047E+06
Average %: 66.8 RMS %: 7.029E+01 Std Dev : 2.196E+01

Figure B11

Program: SMRPC Rev:2.10

Modified Single Mode - Conservative RCS Model
Percent Exceeding 60 NMi Detection Range
Radar: X-Band Target: FF [Avg]
Freq: 10000 MHz FSR: 76.5 NMi
Antenna Height: 66 ft Cut: ON

Long.	Latitude (deg)															
(deg)	-75	-65	-55	-45	-35	-25	-15	-05	05	15	25	35	45	55	65	75
175								81	82	89	82	59	29	13		
165									88	91	84	58	28	12		
155									88	89	86	60	29	16		
145									86	86	84	66	33	20		
135									84	86	81	67	37	27		
125									84	88	78	50	30	24		
115									82	88	69	56				
105									78	78	77					
95								70	79	74	76					
85								60	74		83					
75			23	42	42	70	54			86	84	69				
65			26	40						89	85	77	30			
55				29	47					90	84	75	35	10		
45					66	63			87	88	83	72	44	23		
35						78	84	86	87	89	83	69	54	30	25	
25									84	85	83	67	53	45	24	
15								84	78	74	70	72	54	42	24	
5							88	85	79			59	49	37	21	
-5						79	86	86	81			63	53	36	31	
-15					60	60	56					66	57	24		
-25					69							69	52			
-35					76	82	83				78	75	45			
-45						81	80	83		73						
-55						85			78	68	64					
-65									85	82	73					
-75								84	79	80						
-85									83	80						
-95							86	79	80	80						
-105						86	87	83	80							
-115					81	84	82	79	81	82	74					
-125					67			77	80	83	78	61				
-135					66			83	83	86	77	73	37			
-145								79	86	87	78	69	29			
-155					71	84	86	82	85	87	78	67	27	9		
-165					64	80	84		82	87	78	62	25	13		
-175					55		85		71	87	80	60	28	13		

Counts : 212.0 Sum %: 1.402E+04 (Sum %)^2: 1.030E+06
Average %: 66.1 RMS %: 6.969E+01 Std Dev : 2.205E+01

Figure B12

Program: SMRPC Rev:2.10

Modified Single Mode - Conservative RCS Model
Percent Exceeding 60 NMi Detection Range
Radar: Ku-Band Target: CG-1 [Avg]
Freq: 18000 MHz FSR: 58.1 NMi
Antenna Height: 66 ft Cut: ON

Long.	Latitude (deg)														
(deg)	-75	-65	-55	-45	-35	-25	-15	-05	05	15	25	35	45	55	65	75
175								89	88	93	88	69	42	25		
165									93	94	90	69	42	24		
155									93	93	91	70	43	30		
145									92	92	90	76	47	35		
135									91	92	89	78	52	44		
125									91	93	88	64	44	40		
115									89	93	80	71				
105									86	87	85					
95								81	87	83	83					
85								73	84		89					
75			39	58	58	81	66			91	90	76				
65			40	54						93	91	85	40			
55				40	60					94	91	83	45	20		
45					76	73			92	92	90	82	55	40		
35						87	90	92	92	93	90	79	66	45	43	
25									91	91	90	77	66	61	40	
15								90	87	83	80	82	67	58	39	
5							93	91	87			72	64	54	38	
-5						88	93	92	90			75	64	53	52	
-15					72	72	71					77	71	37		
-25					78							79	66			
-35					85	89	90				85	84	60			
-45						89	87	90		81						
-55						91			85	77	75					
-65									91	88	81					
-75								92	87	87						
-85									90	88						
-95							92	88	89	88						
-105						92	92	90	88							
-115					89	90	89	88	88	89	82					
-125					80			87	88	89	85	71				
-135					79			91	90	91	84	81	53			
-145								89	92	92	85	77	40			
-155					79	90	92	90	91	92	85	75	39	14		
-165					74	87	90		88	91	85	71	38	26		
-175					65		90		79	92	87	70	40	26		

Counts : 212.0 Sum %: 1.599E+04 (Sum %)^2: 1.284E+06
Average %: 75.4 RMS %: 7.782E+01 Std Dev : 1.919E+01

Figure B13

Program: SMRPC Rev:2.10

Modified Single Mode - Conservative RCS Model
Percent Exceeding 60 NMi Detection Range
Radar: Ku-Band Target: CG-2 [Avg]
Freq: 18000 MHz FSR: 58.1 NMi
Antenna Height: 66 ft Cut: ON

Long.	Latitude (deg)															
(deg)	-75	-65	-55	-45	-35	-25	-15	-05	05	15	25	35	45	55	65	75
175								89	88	93	88	69	42	24		
165									93	94	90	68	41	24		
155									93	93	91	70	43	30		
145									92	92	90	76	47	35		
135									91	92	89	78	52	44		
125									91	93	88	64	44	40		
115									89	93	80	71				
105									86	87	85					
95								81	87	83	83					
85								73	84		89					
75			39	58	58	81	65			91	90	76				
65			40	54						93	91	85	40			
55				40	60					94	91	83	45	20		
45					76	73			92	92	90	82	55	40		
35						87	90	92	92	93	90	79	66	45	43	
25									90	91	90	77	66	61	40	
15								90	87	83	80	82	67	58	39	
5							93	91	87			72	64	54	38	
-5						88	93	92	89			75	64	53	52	
-15					72	72	71					77	71	37		
-25					78							79	66			
-35					85	89	90				85	84	60			
-45						89	87	90		81						
-55						91			85	77	74					
-65									91	88	81					
-75								92	87	87						
-85									90	88						
-95							92	88	89	88						
-105						92	92	90	88							
-115					89	90	89	88	88	89	81					
-125					79			86	88	89	85	71				
-135					79			91	90	91	84	81	53			
-145								89	92	92	85	77	40			
-155					79	90	92	90	91	92	85	75	39	14		
-165					74	87	90		88	91	85	71	38	25		
-175					65		90		79	92	87	70	40	26		

Counts : 212.0 Sum %: 1.598E+04 (Sum %)^2: 1.283E+06
Average %: 75.4 RMS %: 7.778E+01 Std Dev : 1.920E+01

Figure B14

Program: SMRPC Rev:2.10

Modified Single Mode - Conservative RCS Model
Percent Exceeding 60 NMi Detection Range
Radar: Ku-Band Target: DD [Avg]
Freq: 18000 MHz FSR: 58.1 NMi
Antenna Height: 66 ft Cut: ON

Long.	Latitude (deg)															
(deg)	-75	-65	-55	-45	-35	-25	-15	-05	05	15	25	35	45	55	65	75
175								88	88	92	87	68	40	23		
165									93	94	90	67	40	22		
155									93	93	91	69	41	28		
145									92	91	90	75	45	34		
135									90	91	88	77	50	42		
125									90	93	87	63	43	38		
115									88	92	79	69				
105									85	86	84					
95								80	86	82	82					
85								72	83		88					
75			37	57	56	80	64			91	89	75				
65			39	52						93	91	84	39			
55				39	58					94	90	82	44	19		
45					75	72			92	92	89	81	54	38		
35						86	90	91	92	93	89	78	65	43	41	
25									90	91	89	76	64	59	38	
15								89	86	82	79	81	66	56	37	
5							93	91	86			70	62	52	36	
-5						87	92	91	89			74	63	51	50	
-15					71	70	69					76	69	36		
-25					77							78	64			
-35					84	88	89				84	83	58			
-45						88	86	89		80						
-55						91			85	76	73					
-65									91	88	80					
-75								91	86	86						
-85									89	87						
-95							91	87	88	87						
-105						92	91	90	87							
-115					88	89	88	87	87	88	81					
-125					78			85	87	88	84	70				
-135					77			90	89	91	83	80	51			
-145								88	91	92	84	77	39			
-155					78	90	91	89	90	91	84	75	38	13		
-165					73	86	89		88	91	85	70	36	24		
-175					64		90		78	91	86	69	39	24		

Counts : 212.0 Sum %: 1.577E+04 (Sum %)^2: 1.254E+06
Average %: 74.4 RMS %: 7.692E+01 Std Dev : 1.958E+01

Figure B15

Program: SMRPC Rev:2.10

Modified Single Mode - Conservative RCS Model
Percent Exceeding 60 NMi Detection Range
Radar: Ku-Band Target: FF [Avg]
Freq: 18000 MHz FSR: 58.1 NMi
Antenna Height: 66 ft Cut: ON

Long.	Latitude (deg)															
(deg)	-75	-65	-55	-45	-35	-25	-15	-05	05	15	25	35	45	55	65	75
175								88	87	92	87	67	40	23		
165									93	94	90	67	40	22		
155									92	93	91	69	41	28		
145									92	91	90	75	45	33		
135									90	91	88	77	50	41		
125									90	93	87	62	42	38		
115									88	92	78	69				
105									85	86	84					
95								80	86	82	82					
85								72	83		88					
75			37	56	56	80	64			90	89	75				
65			38	52						92	90	84	39			
55				39	58					94	90	82	44	19		
45					74	72			92	92	89	81	53	37		
35						86	90	91	92	93	89	78	64	43	40	
25									90	91	89	76	64	59	38	
15								89	85	82	79	81	66	56	36	
5							93	91	86			70	62	51	36	
-5						87	92	91	88			74	63	50	49	
-15					71	70	69					75	69	35		
-25					77							78	64			
-35					83	88	89				84	83	58			
-45						88	86	89		80						
-55						91			84	76	73					
-65									90	88	80					
-75								91	86	86						
-85									89	87						
-95							91	87	88	87						
-105						91	91	89	87							
-115					88	89	88	87	87	88	81					
-125					78			85	87	88	84	69				
-135					77			90	89	91	83	80	50			
-145								87	91	91	84	76	39			
-155					78	90	91	89	90	91	84	74	37	13		
-165					72	86	89		87	91	84	70	36	24		
-175					64		90		78	91	86	69	38	24		

Counts : 212.0 Sum %: 1.572E+04 (Sum %)^2: 1.248E+06
Average %: 74.2 RMS %: 7.672E+01 Std Dev : 1.967E+01

Figure B16